Review

Recent advancements in the measurement of pathogenic airborne viruses

Jyoti Bhardwaj [a], Seongkyeol Hong [b], Junbeom Jang [a], Chang-Ho Han [a], Jaegil Lee [a], Jaesung Jang [a,c,*]

[a] Sensors and Aerosols Laboratory, Department of Mechanical Engineering, Ulsan National Institute of Science and Technology (UNIST), Ulsan 44919, Republic of Korea
[b] LG Electronics, Seoul 08592, Republic of Korea
[c] Department of Biomedical Engineering & Department of Urban and Environmental Engineering, UNIST, Ulsan 44919, Republic of Korea

ARTICLE INFO

ABSTRACT

Air-transmissible pathogenic viruses, such as influenza viruses and coronaviruses, are some of the most fatal strains and spread rapidly by air, necessitating quick and stable measurements from sample air volumes to prevent further spread of diseases and to take appropriate steps rapidly. Measurements of airborne viruses generally require their collection into liquids or onto solid surfaces, with subsequent hydrosolization and then analysis using the growth method, nucleic-acid-based techniques, or immunoassays. Measurements can also be performed in real time without sampling, where species-specific determination is generally disabled. In this review, we introduce some recent advancements in the measurement of pathogenic airborne viruses. Air sampling and measurement technologies for viral aerosols are reviewed, with special focus on the effects of air sampling on damage to the sampled viruses and their measurements. Measurement of pathogenic airborne viruses is an interdisciplinary research area that requires understanding of both aerosol technology and biotechnology to effectively address the issues. Hence, this review is expected to provide some useful guidelines regarding appropriate air sampling and virus detection methods for particular applications.

1. Introduction

Microorganisms such as bacteria and viruses exist in air, which is one of the representative biological aerosols or bioaerosols. These biological particulate matter (PM) comprise viable, nonviable, and/or fragmented organisms, and most of the microorganisms are not pathogenic to humans (Franchitti et al., 2020; Prussin et al., 2015). In this review, viruses that cause respiratory diseases, such as influenza viruses and coronaviruses, are of particular interest among the bioaerosols as they affect both animals and humans significantly and rapidly. During the 2009 pandemic outbreak of the influenza H1N1 virus, more than 17,700 deaths were reported, according to the World Health Organization. The ongoing COVID-19 pandemic has affected approximately 178 million people and resulted in the deaths of more than 3.8 million people worldwide as of June 19, 2021 (https://www.worldometers.info/coronavirus/#countries). The dawn of evolved air-transmissible diseases, such as COVID-19, and their long incubation periods during which the diseases can be transmitted quickly without severe symptoms, as observed in the current pandemic, have increasingly necessitated

direct measurement of viruses from air samples, in addition to the tests on infected hosts.

Bioaerosols are usually detected and/or quantified by collection into liquids or onto solid surfaces, following which they are analyzed using the growth method, nucleic-acid-based techniques, or immunoassays, such as enzyme-linked immunosorbent assay (ELISA) (Cho et al., 2019). Most of the reported reviews on bioaerosol detection by air sampling have focused on allergens, bacteria, and fungi (Šantl-Temkiv et al., 2020; King et al., 2020; Kabir et al., 2020; Huffman et al., 2019), and there are very few reviews on the measurement of viral aerosols. Moreover, recent reviews on airborne viruses have mostly discussed air sampling techniques and their limitations (Pan et al., 2019; Mainelis, 2020); most reviews on viral sensors have focused on liquid-borne viruses rather than airborne viruses (Guliy et al., 2019; Ribeiro et al., 2020; Ji et al., 2020), although airborne viruses show different characteristics when collected and tested at the measurement sites because they are subject to a wide variety of environmental stresses, such as dehydration, reactive oxygen species (ROS) such as ozone, ultraviolet light, and mechanical and/or electrical damage during aerosolization,

* Corresponding author at: Sensors and Aerosols Laboratory, Department of Mechanical Engineering, Ulsan National Institute of Science and Technology (UNIST), Ulsan 44919, Republic of Korea,.
E-mail address: jjang@unist.ac.kr (J. Jang).

airborne transport, and sampling.

Herein, we present a review of the recent advancements in the measurement of airborne pathogenic viruses or viruses that can infect hosts through transmission by air and cause respiratory diseases, since 2009 along with their limitations and with additional focus on the SARS-CoV-2 and influenza viruses. We also list the damage caused to airborne viruses during sampling and their effects on the measurements, with the aim of providing guidelines for the sampling and detection methods that are appropriate and compatible with each other. Most air sampling processes can cause damage to the sampled viruses physically and/or biologically either globally or locally; hence, specific analytical tools are required to determine the particular states of the bioaerosols, such as infectivity. For instance, nucleic-acid-based techniques do not require the surface proteins of sampled viruses to be intact for detection; hence, the effects of damage to the surface proteins during sampling are minimal.

In this review, some basic properties of airborne pathogenic viruses, such as their general structure, disease transmission routes, size range of human-generated viral aerosols, resistance to environmental stress, and indoor and outdoor viral concentrations, are introduced. Further, a general procedure for measuring airborne viruses, enrichment strategies for the viral aerosol particles, and some air samplers such as inertia-based, electrostatic, and condensation-based samplers are presented. Lastly, measurement of viruses collected with air samplers are discussed with respect to using the plaque assay, nucleic-acid-based amplification method, immunoassays, affinity-based advanced measurement, and optical detection techniques.

2. Basics of airborne pathogenic viruses

2.1. General structure of the virus

Unlike bacteria, viruses cannot reproduce by themselves and depend on the host cells for propagation. The genome of a virus consists of deoxyribonucleic acids (DNA) or ribonucleic acids (RNA), which may be circular (C) or linear (L) and double stranded (ds) or single stranded (ss). In the case of ssRNA (positive or negative) viruses, the positive sense viral RNA (e.g., coronaviruses) is similar to the mRNA, whereas the negative sense viral RNA (e.g., influenza viruses) is complementary to the mRNA and must be replicated to the mRNA using RNA polymerase (Gelderblom, 1996). The dsDNA viruses also have a sense strand acting as the mRNA and an antisense strand complementary to the mRNA; however, the ssDNA viruses are first made into the double stranded form using DNA polymerase before mRNA synthesis (Gelderblom, 1996) (Fig. 1). Viral nucleic acids are surrounded by a protein coat or capsid

comprising multiple copies of a single protein or several proteins. The combination of a capsid and the internal nucleic acids is called a nucleocapsid or nucleoprotein (NP), which functions as a shell to protect the viral genome. In some viruses, the nucleocapsids are covered with outer membranes or envelopes, which consist mainly of phospholipid bilayers and contain one or two types of virus-encoded glycoproteins, such as hemagglutinin (HA) for the influenza virus. Glycoproteins are receptor-binding proteins that help in binding to the host cells, and the internal domains of the host cells interact with the viral matrix protein (MP), which functions as a bridge between the glycoproteins and NP (Harvey et al., 2000). Depending on the existence of the outer membrane, viruses are categorized into two groups: enveloped and non-enveloped viruses (Fig. 2).

Bacteriophages are viruses whose hosts are bacteria. MS2 bacteriophages, whose host is *Escherichia coli*, are extensively used as surrogates for many air-transmissible pathogenic viruses in bioaerosol studies because they have a similar structure; they are also safer and more convenient to use for lab-scale experiments. Pathogenic viruses often need to be inactivated before aerosolization in experiments, and UV-inactivated viruses usually do not affect detection via polymerase chain reaction (PCR) (Myatt et al., 2003; Bender et al., 1995) and immunoassays (Wang et al., 1995), which additionally helps improve the safety of experiments involving these viruses.

Viruses primarily differ from bacteria by their lack of ribosomes, adenosine triphosphate (ATP), and cellular machinery for reproduction (Cossart and Helenius, 2014). Viruses are visible only under electron microscopes, and viral enrichment via normal centrifuging is generally not effective owing to their small size, whereas bacteria are larger in size and visible under a light microscope. Because of these reasons, several techniques like ATP bioluminescence and fluorescent assays may not be effective for detecting viruses.

2.2. Disease transmission routes and minimum infective dose

Viruses causing respiratory diseases are transmitted in several ways, and several examples of such viruses and their minimum infective doses (MIDs) and survival times are summarized in Table 1. The typical modes of transmission are droplet, contact (direct and indirect), and aerosol transmission (Fig. 3). An aerosol particle size of 5 μm is considered as the boundary between droplet and aerosol transmission modes, as suggested by the US Centers for Disease Control and Prevention (CDC). Recently, the US CDC has categorized the transmission routes of SARS-CoV-2 in three ways: inhalation of fine droplets and aerosol particles, deposition of droplets on mucous membranes, and touching mucous membranes with contaminated hands (CDC, 2021).
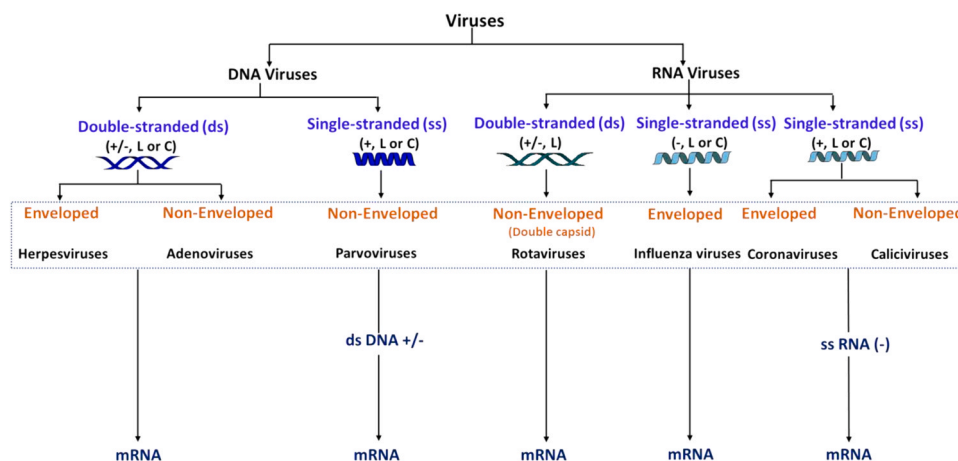

Fig. 1. Classification of viruses and examples. C: circular, L: linear, +: sense strand, -: antisense strand. Image modified from Rosenthal et al. (2011).
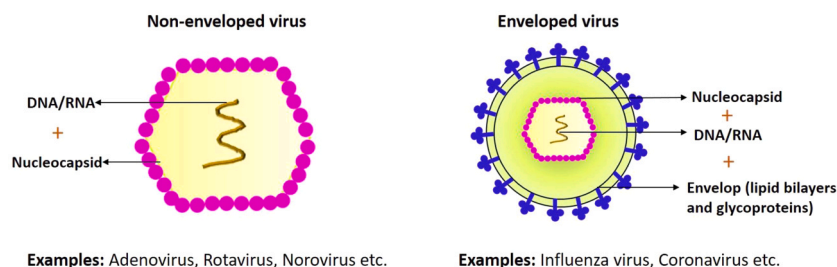
Fig. 2. Structures of non-enveloped and enveloped viruses.

Table 1
Minimum infective doses of respiratory disease viruses for humans with their sizes and survival times. S: spherical, I: icosahedral, I-S: icosahedral spherical, TCID$_{50}$: fifty-percent tissue culture infective dose, E: enveloped, NE: non-enveloped.

| Viruses	Shape	Type	Size (nm)	Minimum infective dose (TCID$_{50}$)		Survival time			References
				Nasal drop	Aerosol	Non-porous	Porous	Skin	
Influenza A virus	S	E	80–120	10^3 (H1N1)	0.6–3.0 (H2N2)	24–48 h	8–12 h	15 min	(Karimzadeh et al., 2021; Yezli and Otter, 2011)
Respiratory syncytial virus (RSV)	S	E	30–40	30–40 (Type−1)	–	6 h	30–45 min	20 min	(Karimzadeh et al., 2021; Vasickova et al., 2010)
Parainfluenza virus	S	E	150–250	–	–	10 h	4 h	1 h	(Walther and Ewald, 2004)
Adenovirus	I	NE	90–100	35	0.5	–	–	–	(Karimzadeh et al., 2021)
Coronavirus	S	E	80–160	13 (HCoV-229E)	–	3–4 days	30 min–7 days	9 h	(Watanabe et al., 2010)
Rhinovirus	S	NE	30–50	0.032	0.68	> 25 h	1–24 h	1–3 h	(Ikonen et al., 2018; Yezli and Otter, 2011; Walther and Ewald, 2004)
Rubella virus	S	E	60–70	0.2		–	–	–	(Knudsen, 2001)
Coxsackievirus	I-S	NE	30	6	28–34	–	–	–	(Karimzadeh et al., 2021)
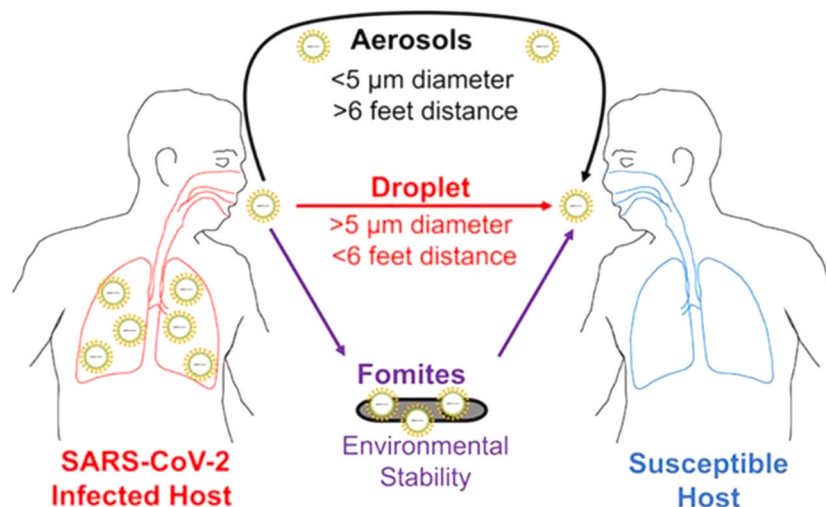
Fig. 3. Transmission routes of COVID-19.
Image modified from Galbadage et al. (2020).

Droplet-based transmission refers to the condition where virus-laden droplets move directly thought the air from an infected person to the respiratory system of another. Particles greater than 5 μm are quickly removed from the air by collision or gravitational sedimentation, and most of them are collected at the upper respiratory tract, making it difficult for them to reach the lower respiratory tract (Brown et al., 2013). Airborne (aerosol) transmission is caused by the inhalation of smaller respirable-sized aerosols containing viruses. There are several pathogenic viruses that can be transmitted from person to person through the air, such as the influenza virus (flu), varicella-zoster viruses (chicken pox), rubella viruses (measles), and SARS-CoV-2 (COVID-19)

(Tellier et al., 2019; Nissen et al., 2020). These airborne viruses can also travel on solid particles, such as dust and skin flakes, or in aerosol droplets. Large droplets containing such viruses can also accumulate on certain surfaces, commonly called fomites, thereby contributing to contact transmission. In such cases, infection occurs by touching the mouth and/or nose with virus-contaminated hands after contact with fomites.

The survival times of airborne viruses on surfaces differ based on whether the surfaces are nonporous (e.g., plastic, stainless steel, glass) or porous (e.g., papers and clothes) (Alidjinou et al., 2019). Nonporous surfaces are major contributors to disease transmission (Ikonen et al.,

2018) since the survival times of airborne viruses on them have been observed to be much longer than those of porous surfaces (Table 1). The SARS-CoV-2 virus was observed to be viable for 3 h in aerosols, with decrease in infectious virus concentration from $10^{3.5}$ to $10^{2.7}$ $TCID_{50}$ per liter of air (van Doremalen et al., 2020), but this could be less in outdoor conditions depending on damage to the virus from environmental stress (Chirizzi et al., 2021). The SARS-CoV-2 strain was observed to be more stable on stainless steel and plastic than on cardboard and copper, and the virus was viable for up to 72 h after being deposited on the surfaces although the number of viable viruses greatly decreased (van Doremalen et al., 2020).

The MIDs of several pathogenic airborne viruses, including the influenza virus, coronaviruses, adenoviruses (Karimzadeh et al., 2021; Yezli and Otter, 2011), and rubella virus (Knudsen, 2001), in humans have been reported (Table 1), which are closely related to the limits of detection (LODs) of the corresponding sensors. The measurement of the MID in human studies requires administration of the virus via nasal drops that can cause infection in the upper respiratory tract or by aerosols that can cause both lower and upper respiratory tract infections (Yezli and Otter, 2011). Although the MID of SARS-CoV-2 in humans needs more research, it is expected to be approximately 100 virus particles (Karimzadeh et al., 2021). The only human study regarding a coronavirus has been reported for HCoV-229E and its MID is 9 PFU. Furthermore, if aerosol transmission is the dominant mode, then the MID would be lower (Karimzadeh et al., 2021).

2.3. Size range of human-generated viral aerosols and their infectivity studies

An infected person can emit viral aerosols through the saliva and mucus by sneezing, coughing, breathing, speech, etc. Because of the aerodynamic behaviors of viral aerosols, their propagation through air and deposition in the respiratory tract depend heavily on their aerodynamic particle sizes, so it is of critical importance to know the size distributions of viral aerosols for preventing the spread of viral diseases. The particle size distributions in air are also determined by aerosolization of the viral particles through the generation principle, nebulization media, etc., all of which are closely related to the surface tension of the fluid lining the respiratory tract and its rupture in humans (Wilson et al., 2020).

As the sizes of the generated aerosol particles increase, the number of microbial particles may also increase, and solute components around these particles might offer protection from the surrounding environment, thereby maintaining infectiousness; however, these particles have shorter times to remain airborne. On the other hand, if the particles are smaller, they have a higher probability of reaching the lower respiratory tracts of the victims, where the infections may be of greater severity as they can damage lung function and affect morbidity and fatality (Gralton et al., 2011). In fact, aerosol-based infections require less doses, e.g., ~100 times less, than droplet-based infections (Tellier, 2009). Moreover, the spike proteins of SARS-CoV-2 viruses specifically adhere to the angiotensin-converting enzyme-2 (ACE-2) receptors, which have significantly higher presence on the alveolar surfaces than bronchial surfaces, and the alveolar surfaces have thinner lining fluids that allow easier exposure of the ACE-2 receptors (Wilson et al., 2020).

Viruses usually have a size range of 25–400 nm. A single virus particle can exist in air (Hogan et al., 2005) and can aggregate with other particles to form larger particles during aerosolization or transmission. The particle sizes can vary depending on the sizes of the initial droplets as well as the concentrations of the virus and solute in the droplets rather than the sizes of the viruses themselves (Verreault et al., 2008). Solutes can be organic or inorganic substances, proteins, salts, etc., and higher concentrations of solutes enable more agglomeration upon evaporation of moisture to form larger particles. Water droplets of sizes as large as 50 μm evaporate immediately upon expulsion into the air and can desiccate completely within 2–3 s, and a water droplet of 10 μm diameter evaporates within 0.5 s at 50% relative humidity (RH) at 293 K (Hinds, 1999).

The size distributions of droplets generated from healthy people during breathing, coughing, sneezing, and speech and from those with respiratory infections range from submicrometer to several tens of micrometers (Gralton et al., 2011; Fronczek and Yoon, 2015). The size distributions of viral aerosols generated from breathing and coughing by patients with various respiratory infections showed high similarities, and size proportions < 5 μm were dominant (Fennelly, 2020). Table 2 shows studies on the particle size distributions of viral aerosols emitted during human respiratory activities or measured in hospitals. Most of these measurements were conducted by PCR rather than a growth technique because it is difficult to collect infectious airborne viruses effectively and without damage during sampling, in addition to the constraint that airborne virus concentrations are generally very low. Milton et al. (2013) observed from the coughing of people infected with seasonal influenza that particles of sizes 5 μm or less have 8.8 times more viral copies than those greater than 5 μm using a slit sampler with condensation and quantitative real-time PCR (qPCR) measurements. Viral RNAs were detected at size ranges of 0.65–4.7 μm and > 4.7 μm from approximately 80% and 58% of the participants (children and adults) with respiratory symptoms, respectively, through breathing and coughing (Gralton et al., 2013).

Airborne viruses were also measured in a hospital having patients with respiratory infections. A significant number of infective particles in the air of pediatric wards and intensive care units with infants having respiratory syncytial virus infections had an aerodynamic diameter of 4.7 μm or less (Binder et al., 2020; Hill et al., 2013; Kulkarni et al., 2016). The particle size distribution of the SARS-CoV-2 RNAs measured at hospitals in Wuhan had two peaks at the size ranges of 0.25–1.0 μm and > 2.5 μm (Liu et al., 2020). On the other hand, in other hospitals, SARS-CoV-2 RNAs were found to have size ranges of 1–4 μm and > 4 μm when sampled with the National Institute for Occupational Hygiene (NIOSH) BC-251 samplers; however, no RNAs were found in the range of < 1 μm when sampled with polytetrafluoroethylene (PTFE) filters (Chia et al., 2020).

In addition to the measurement of RNAs from collected airborne SARS-CoV-2 samples, the infectivity of the viral particles was investigated (Binder et al., 2020; Santarpia et al., 2020; Dumont-Leblond et al., 2020; Lednicky et al., 2020). Santarpia et al. (2020) collected air samples from the rooms of patients in a hospital and detected infectious SARS-CoV-2 virions in the size ranges of < 1 μm and 1–4 μm via growth. They used a NIOSH sampler with a gelatin filter in the final stage and observed intact viruses in the filter (<1 μm) using a transmission electron microscope (TEM). However, all viral cultures were negative for the air samples collected by gelatin filters for 6 or 18 h (Dumont-Leblond et al., 2020), which may be because gelatin filters normally maintain their moisture for a short period of time. Lednicky et al. (2020) successfully detected infectious airborne SARS-CoV-2 (6–74 $TCID_{50}$ per liter of air) using condensation-based samplers, which offer higher biological recovery for viruses compared to dry-phase samplers. Infectious influenza viruses were found in cough aerosols, mostly in the aerodynamic particle size range of < 4 μm (75% from 1 to 4 μm and 20% from <1 μm) (Noti et al., 2012). The differences in these measurements may also be attributed to differences in the sizes of the generated viral particles and/or different air sampling and extraction methods used.

2.4. Resistance of airborne viruses to environmental stress

The stability of airborne viruses depends on environmental stresses such as temperature, RH, ROS, and UV light as well as the virus structure (Spieksma et al., 1997). Non-enveloped viruses, which do not have external lipid layers, usually have highly resistant capsid proteins to both solvents and hydrophilic disinfectants (Sakudo et al., 2011). Small, non-enveloped viruses are most stable and resistant to most disinfectants and environmental stresses, such as UV light (Fig. 4). Large,

Table 2

Studies on the size distribution of human or naturally generated viral aerosols. PTFE: polytetrafluoroethylene; OPC: optical particle counter; LPM: liters per min; qPCR: quantitative (real-time) polymerase chain reaction; NIOSH: National Institute for Occupational Safety and Health; qRT-PCR: quantitative reverse transcription-PCR; ddPCR: droplet-digital-PCR; TCID$_{50}$: fifty-percent tissue culture infective dose; PC: polycarbonates; TEM: transmission electron microscope.

References	Target		Sampling		Measurement	
	Virus	Generation or place	Sampler	Flow rate (LPM)	Method & Result	Comment
(Fabian et al., 2008)	Influenza virus A (H3) & B	Tidal breathing by patients	PTFE filters	28.3	OPC 0.3–0.5 μm: 70%; 0.5–1 μm: 17%; 1–5 μm: 13%; > 5 μm: < 0.1% qPCR Exhaled influenza RNA generation rate: 3–20 RNA/min	
(Lindsley et al., 2010)	Influenza A virus	Coughing by patients	NIOSH sampler; BioSampler	NIOSH sampler: 3.5; BioSampler: 12.5	qPCR < 1 μm: 42%; 1–4 μm: 23%; > 4 μm: 35%	The viability of virus collected with the BioSampler was about 4 times higher than that with the NIOSH sampler (dry phase).
(Milton et al., 2013)	Influenza virus A & B	Coughing by patients	Slit sampler with moisture condensation	130	qRT-PCR ≤ 5 μm: 89.8%; > 5 μm: 10.2%	About 50% of the infectious virus was lost during the concentration step.
(Gralton et al., 2013)	Influenza A & B; Parainfluenza 1–3; Human metapneumovirus; Human rhinovirus	Breathing and coughing by participants with respiratory symptoms	Andersen sampler	28	RT-PCR Portion of patients generating viral particles (by breathing) 0.65–4.7 μm: 81%; > 4.7 μm: 58%; (by coughing) 0.65–4.7 μm: 82%; > 4.7 μm: 57%	
(Blachere et al., 2009)	Influenza A	Emergency department of a hospital	NIOSH sampler	3.5	qPCR < 1 μm: 4%; 1–4 μm: 49%; > 4 μm: 46%	
(Leung et al., 2016)	Influenza A	Isolation rooms of patients in a hospital (Hong Kong)	NIOSH sampler	3.5	# of RT-PCR positive samples < 1 μm: 0/5; 1–4 μm: 1/5; > 4 μm: 4/5	Influenza virus RNA recovery was associated with decreasing temperature and increasing relative humidity.
(Kulkarni et al., 2016)	Respiratory syncytial virus	Pediatric wards and intensive care units with infected babies (London)	Andersen sampler	28.3	Plaque assay 1.1–4.7 μm: 65–67% of total collected sample	Detection of high virus concentrations may be due to suctioning of the endotracheal tube.
(Liu et al., 2020)	SARS-CoV-2	Hospital indoors (Wuhan)	Sioutas cascade impactor; Filters	Sioutas impactor: 9; Filters: 5	ddPCR Peak RNA concentration in the protective-apparel removal room (copies/m^3) 0.25–0.5 μm: 40; 0.5–1.0 μm: 9; > 2.5 μm: 7	Re-aerosolization of submicron viral particles from clothing was assumed.
(Chia et al., 2020)	SARS-CoV-2	Infection isolation rooms of patients in a hospital (Singapore)	NIOSH sampler	3.5	qPCR RNA concentrations (copies/m^3) 1–4 μm: 1384 & 916; > 4 μm: 2000 & 927	The non-detection of virus in particles < 1 μm was assumed to be due to low extraction efficiency from filters compared with centrifuge tubes.
(Binder et al., 2020)	SARS-CoV-2	Rooms of patients in a hospital (North Carolina)	NIOSH sampler	3.5	# of qRT-PCR positive samples < 4 μm: 2/195; > 4 μm: 1/195	No infectious virus was cultured from aerosol samples, which may be due to long-term (4 h) dry-phase sampling.
(Santarpia et al., 2020)	SARS-CoV-2	Rooms of patients in a hospital (Nebraska)	NIOSH sampler with a gelatin filter (<1 μm)	3.5	Mean qRT-PCR equivalent TCID$_{50}$/m^3 < 1 μm: 1.2–7.4; 1–4 μm: 0.3–0.7; > 4.1 μm: 1.4–4.0 # of significant viral growth sample (p-value) < 1 μm: 3/6 ($p < 0.05$); 1–4 μm: 2/6 ($p < 0.1$); > 4.1 μm: 0/6	Gelatin filter in the final stage of the sampler may help preserve intact virus (observed by TEM) during sampling.
(Dumont-Leblond et al., 2020)	SARS-CoV-2	Rooms of patients in a hospital (Quebec)	Gelatin filter; PC filter; SASS 3100	Filters: 10; SASS 3100: 300	qRT-PCR RNA concentrations (copies/m^3) (Sampling time: 6 h)	Non-detection in SASS 3100 may be due to short sampling time (15 min), high sampling velocity, high-frequency

Table 2 (*continued*)

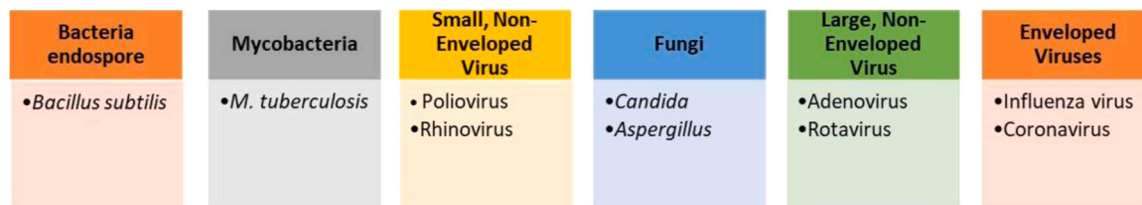| References	Target		Sampling		Measurement	
	Virus	Generation or place	Sampler	Flow rate (LPM)	Method & Result	Comment
					Gelatin filter: 63.79 & 208.33; PC filter: 9.86 & 335.42 (Sampling time: 18 h) Gelatin filter: 23.25 & 187.5; PC filter: 270.83 & 514.17 All viral cultures were negative.	vibration, and exposure to detergent during the extraction.

Fig. 4. Descending order of resistant pathogens (viruses, spores, fungi etc.) to UV light, which is one of the most common environmental stresses, and disinfectants. Image modified from Masri et al. (2013).

non-enveloped viruses, such as rotaviruses, are less resistant and their larger size (70–100 nm) renders them more vulnerable to environmental stress.

Influenza viruses and coronaviruses are typical examples of large enveloped viruses that are composed of capsid proteins surrounded by lipid bilayers containing surface proteins, which help in interactions with the host cells (Sakudo et al., 2011). The lipid layers of the enveloped viruses were susceptible to most disinfectants and UV light, and other physical and biological stress generated during aerosolization (using a Collison nebulizer) and sampling (AGI-30 liquid impinger) might affect the viruses in comparison with the MS2 viruses (Christopher and GwangPyo, 2007). It was observed that coronaviruses (MHV: murine hepatitis virus) were more sensitive to 254 nm UV-C light than adenoviruses (Serotype 2) (only 12% of the coronaviruses survived after exposure to 0.599 mJ/cm^2, whereas 33% of the adenoviruses survived after exposure to 2.608 mJ/cm^2) (Christopher and GwangPyo, 2007). Although it is known that all pathogens require different UV-C irradiation doses for successful inactivation, a family of enveloped viruses, such as the influenza virus (2 mJ/cm^2), requires relatively low fluency of UV-C light (3–14 mJ/cm^2) than a family of non-enveloped viruses, such as adenoviridae (98–222 mJ/cm^2) and polyomaviridae (235–364 mJ/cm^2) (Khalid Ijaz et al., 2020).

RH and temperature are also main environmental factors that can affect the stability and viability of a virus in air. Previous studies suggested that non-enveloped viruses are able to survive longer at high RHs (70–90%) while enveloped viruses survive longer at low RHs (<30%) (Božič and Kanduč, 2021); however, these observations are not always consistent. Moreover, enveloped viruses are observed to be more stable at low temperature and susceptible to damage at high temperature due to dysfunction of their phospholipid bilayers (Price et al., 2019). Temperature above 60 °C can inactivate most DNA and RNA viruses although DNA viruses are more stable than RNA viruses. Surrounding materials such as mucus or saliva can also affect because they can provide insulation to viruses and prevent from drying under extreme environmental conditions (Tang, 2009).

Viral infectivity can be expressed by the ratio of viral copies to PFUs, which can vary significantly depending on the type of virus, air sampler, environmental stress and culture conditions (Yang et al., 2011). For influenza viruses (H1N1 and H3N2) collected with air samplers, the ratios of 7.5×10^3–1.0×10^4 copies/PFU were reported and were higher for those collected in the nebulizer, that is before aerosolization, suggesting infectivity loss during aerosolization and sampling in addition to environmental stress (Bekking et al., 2019), which needs to be considered when assessing the effects of environmental stress on the stability of airborne viruses.

2.5. Outdoor and indoor virus concentrations

Studies on concentrations of airborne viruses are limited (Yang et al., 2011; Prussin et al., 2014; Whon et al., 2012), and quantifying the total virus concentration in the air is challenging because effective capture of viruses from the air is difficult; further, viruses lack a conserved common gene that can be used for qPCR quantification, unlike bacteria (Prussin et al., 2015). Whon et al. collected viral aerosols using an impinger with a water jet pump and reported the seasonal fluctuations in outdoor concentrations of viruses, which ranged from 1.7×10^6 to 4.0×10^7 viruses m^{-3} in Korea with fluorescence staining and confocal laser scanning microscopy (Whon et al., 2012).

The average concentration of airborne influenza A viruses collected indoors at a healthcare center and measured with qPCR during the 2009–2010 flu season was 1.6×10^4 genome copies m^{-3}, equivalent to 35.4 ± 21.0 TCID$_{50}$ m^{-3} (Yang et al., 2011). The number of influenza A viruses exhaled by humans were measured to be less than approximately 10^3 for 30 min (Milton et al., 2013). Airborne SARS-CoV-2 samples were collected from hospital rooms of infected patients using NIOSH BC-251 samplers, and the total concentrations in air measured using qPCR varied between 1.84×10^3 and 3.38×10^3 RNA copies (virions) m^{-3} (Chia et al., 2020). Hu et al. (2020b) also collected aerosol samples from hospitals, university, hotels, residential communities, gardens, and greenways in Wuhan, China, using a centrifugal aerosol-to-hydrosol sampler with a 50% aerodynamic equivalent cut-off diameter of 0.8 μm at 400 liters per minute (LPM) and performed analyses using PCR. The concentrations of SARS-CoV-2 in the positive samples collected from intensive care units and computerized tomography rooms were 1.11×10^3 to 1.12×10^4 RNA copies m^{-3} (Hu et al., 2020b). However, the samples collected from other areas of the hospitals, such as the rest areas and passageways, were all negative, which may be attributed to good ventilation (Hu et al., 2020a). The outdoor viral

concentrations in the positive samples were smaller and varied from 0.89×10^3 to 1.65×10^3 RNA copies m^{-3} (Hu et al., 2020b).

3. General measurement procedure of airborne viruses

The measurement methods for bioaerosols can be largely divided into two groups. The first involves measuring the physical/biological information of the aerosols without air sampling, and the second involves measuring such information following air sampling. In the former method, the auto-fluorescence spectra of microbial particles are commonly measured to enable real-time detection; however, this approach has a limitation that it is difficult to identify and quantitatively measure particular targets in the presence of non-targets. Moreover, this approach is not effective for detecting airborne viruses as the amount of fluorescence from viruses is usually very small compared to those from molds and bacteria.

The latter method can be used for airborne viruses and involves two steps (Fig. 5). First, the viral aerosol particles need to be directly collected into liquids or onto solid surfaces before suspending the particles in liquids, which is called hydrosolization. Since most biological analysis methods, such as cultures, molecular microbiological analyses, and ELISA, are based on activity and reaction in the liquid phase, hydrosolization of the viral aerosols is essential. Measurement techniques, including the growth technique, nucleic-acid-based techniques such as qPCR, and immunoassays such as ELISA, are subsequently applied to detect and/or quantify the viral particles.

3.1. Enrichment strategies of viral aerosol particles

Since the concentrations of viruses in air are generally very low, the measurement system needs effective concentration techniques for the viruses without causing physical/biological damage, and/or the LOD of the measurement system should be low enough to detect the virus concentration robustly and stably. The minimum detectable virus concentration in air is related to the enrichment ratio (ER) of a sampler and the LOD of the measurement system (Bhardwaj et al., 2020), which is given by the following formula: $C_V \times \text{ER} \geq \text{LOD}$, where C_V and LOD represent the detectable virus concentration in air (number of viruses or TCID$_{50}$ cm^{-3}) and LOD of a viral sensor (number of viruses or TCID$_{50}$

mL^{-1}), respectively. The ER can be expressed as $(Q \times \eta)/\left(\frac{V_m}{t}\right)$, where Q, η, V_m, and t represent the volume flow rate (cm^3/min) of the sampler, overall physical collection and biological preservation efficiency from the air flow at the inlet to a sampling medium, volume of a sampling medium (mL), and sampling time (min), respectively, where the medium can be either stagnant or flowing.

The effective concentration can be obtained by adopting high ER values, that is, large flow rates, high overall physical collection and biological preservation efficiencies, small volume of sampling media, and long sampling periods; however, sampling with a large flow rate can diminish the biological preservation efficiencies of particular viruses in the case of inertia-based samplers (Hong et al., 2016). Moreover, the physical collection and biological preservation efficiencies may depend on the measurement technique to be used afterwards. For example, if a viral culture is used for quantification, the biological preservation efficiency must be considered. However, when immunoassays are used for quantification, the biological preservation efficiencies for the particular proteins used in the assay must be considered.

This enrichment method can be broadly divided into three types: gas phase, aerosol-to-hydrosol process, and liquid phase. One of the most common aerosol concentration methods in air is to use a virtual impactor, which separates the incoming aerosol particles into two channels, major and minor, depending on their sizes. Smaller particles follow the turning flow into the higher flow channel (major) and larger particles travel straight into the smaller flow channel (minor) because of their larger inertia, where the minor flow usually comprises ~10% of the inlet flow rate and the major flow comprises the other of the inlet flow rate. Most of the larger particles can be guided into the minor flow to increase the airborne particle concentration in the minor flow channel, usually by approximately 100 times or more using two stages (Ho, 2011). However, the overall efficiency to transfer aerosol particles from the nozzle inlet to the minor flow channel and the ER decrease as the particle size decreases.

The next method to increase airborne particle concentration in the collection medium involves guiding the airborne particles into a small amount of the medium (Hong et al., 2016; Kim et al., 2020a). Hong et al. (2016) presented the electrostatic aerosol-to-hydrosol concentration of airborne viruses onto stagnant 0.5 mL media, and the ER can increase to 450,000 at a flow rate of 12.5 LPM for 60 min.
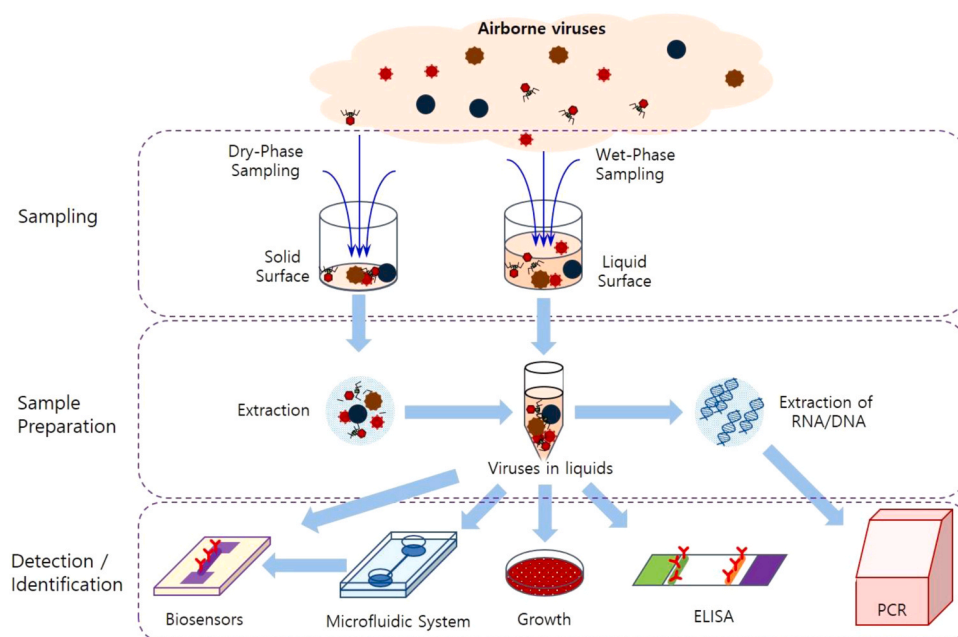

Fig. 5. General procedures of airborne virus measurements: sampling and identification.

Particle enrichment can also be performed after collection into the sampling medium to increase the sample concentration. Specifically, AC electrokinetic methods such as electroosmosis and dielectrophoresis (DEP) have attracted much attention for concentrating specific particles prior to detection (Han et al., 2018, 2019). A more detailed review of this topic is available elsewhere (Salari and Thompson, 2018). Kim et al. (2020b) employed an enrichment technique with Concanavalin A-coated magnetic particles, which can adsorb particular terminal carbohydrates of viruses and bacteria, for air-sampled biological particles.

4. Air samplers

The ideal microbial air sampler should be able to collect representative biological particles of all sizes in a particular space without loss of microbial status and physical collection of microorganisms. The sampler should also be compatible with subsequent microbial analyses. Rapidity (or high sampling flow rate), portability, and high values of ER are also some of the other required properties. However, the present microbial air samplers meet only some of these requirements based on sampling principles, and these requirements are often contradictory to each other considering that viral concentrations in air are very low. For example, high flow-rate operation is desired for surveillance of large volumes of air for many cases, and if the sampling flow rates are high enough to ensure high enrichment and rapid sampling, as in conventional inertia-based samplers such as impactors, the viral aerosol particles may be damaged, and it may be difficult to conduct rapid or on-site analyses. If the sampling flow rate is decreased to reduce damage to the collected airborne microbial particles, sampling large volumes within a given period would be difficult, thereby disabling certain applications. In the inertia-based samplers, the physical collection efficiency generally decreases as the flow rate decreases; the physical collection also depends significantly on particle size, so particles of all sizes cannot be equally collected. Portability can also provide flexibility with respect to the measurement location despite less sampling flow rate and reliable measurements considering that the aerosol densities of bioaerosols are not uniform even in a small room, thus resulting in different results depending on the location of the sampler. Therefore, it may be desirable or realistic to make meaningful sampling by prioritizing the parameters, e.g., particle size range, flow rate, sampling time, physical collection efficiency, portability, biological preservation, and ER, according to the measurement objectives.

In this section, we introduced several air sampling technologies that have attracted attention, such as condensation-based sampling and electrostatic particle concentrator, as well as traditional sampling techniques, such as filters, impactors, impingers, and electrostatic precipitators (ESPs), to collect airborne viruses. Although the US NIOSH has

recommended Andersen samplers for bacterial and fungal sampling, there are no standard sampling methods for airborne viruses (Rahmani et al., 2020). Fig. 6 and Table 3 show the air samplers that have been used in viral aerosol studies and their characteristics, respectively. The measurement of artificially generated viral aerosols and the causes affecting the physical/biological efficiencies in the samplers are also reviewed (Table 4).

4.1. Air samplers: impactors and impingers

In impactors, the airborne particles are accelerated through a nozzle by a vacuum pump and collide with the collection plate, which typically consists of a filter material or agar plate, via deviating streamlines owing to their large momenta (Marple and Willeke, 1976; William et al., 2017). If the plate is a filter, it can be washed after sampling, and the washed solution can be analyzed (Appert et al., 2012; Alonso et al., 2017). If the collection plate incorporates agar, it may be either washed to collect the particles for further analysis (Zhao et al., 2014) or transferred directly to an incubator, thereby simplifying the process and reducing sample losses (Tseng and Li, 2005).

Impaction-based samplers are widely used for sampling large-sized bioaerosols, such as bacteria and fungi, because the collection efficiencies for such particles are high and these devices are relatively easy to use. The collection efficiency of the sampler is a function of the Stokes number (Stk), which is proportional to the square of the particle diameter, particle density, and nozzle velocity and inversely proportional to the nozzle diameter. Larger particles with higher Stokes numbers adhere to the collection plate while the smaller particles flow along the streamline and exit without collection. The particle size at which 50% collection efficiency is obtained is called the cut-off diameter (d_{50}). In general, the smallest cut-off diameter of an impactor is known to be about 0.2–0.3 μm, which is sufficient to sample airborne bacteria but insufficient to sample single virus particles. Impactors with smaller nozzle diameters for higher acceleration enable collection of smaller particles (Marple and Willeke, 1976), but such impactors are difficult to manufacture and the resulting sonic flow may damage the virus particles (Pan et al., 2019). Bioaerosol particles undergo mechanical impact with the collection plates in these samplers, which can affect their biological intactness and hence their detection. For example, the integrity of a virus can be damaged by high shear forces and dehydration during impaction (Zhao et al., 2014).

The sampling mechanism of an impinger is similar to that of the impactor, and the primary difference between these devices is that the collection place of the impactor is replaced with a liquid reservoir in the impinger. One of the advantages of using an impinger is that it shows good biological recovery compared to the impactor; hence, the
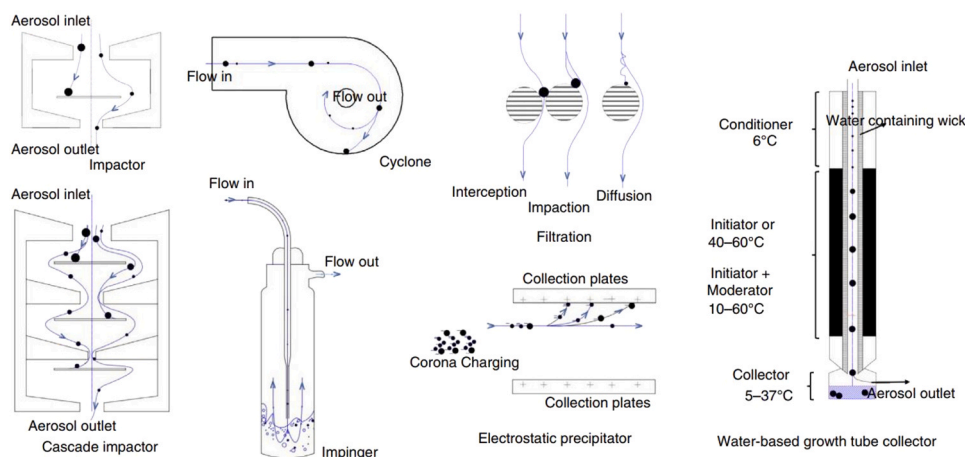

Fig. 6. Schematics of several air samplers used in studies on airborne viruses (Pan et al., 2019).

Table 3

Air samplers used in studies on airborne viruses and their characteristics. PTFE: polytetrafluoroethylene; PC: polycarbonates.

	Filters	Impactors	Impingers	Cyclones	Electrostatic samplers	Condensation-based samplers
Main principle	• Interception • Inertial impaction • Diffusion • Gravitational settling • Electrostatic attraction	• Inertial impaction on a solid surface	• Inertial impingement on a liquid surface	• Centrifugal & inertial impaction on a liquid (wet type) or solid (dry type) surface	• Electrostatic attraction of pre-charged particles on a liquid (wet) or solid (dry) surface	• Size increase via condensation and then impaction or impingement on a liquid (wet type) or solid (dry type) surface
Devices	• PTEF, PC filters • Gelatin filters	• Slit sampler • Andersen sampler	• AGI-30 • SKC BioSampler	• Dry/wetted-wall cyclone sampler	• Large volume sampler (LVS)	• BioSpot-VIVAS
Advantages	• Simplicity • High collection efficiency	• Size-selective sampling • High flow rate	• Relatively high biological recovery	• High flow rate	• High collection efficiency over a wide range of particle size	• High collection efficiency • High biological recovery
Disadvantages	• Desiccation of samples • Incompatibility with viability analysis	• Low efficiency for submicron particles • Low biological recovery	• Low efficiency for submicron particles • Fragile container	• Low efficiency for submicron particles • Relatively low biological recovery	• Low sampling flow rate • ROS generation	• Low sampling flow rate • Bulkiness and complexity
Main sources of damage and viability losses	• Dehydration and desiccation of biological particles	• High impaction of biological particles	• High impaction of biological particles	• High impaction of biological particles	• High electric field intensity and corona charging	• High temperature during sampling

BioSampler®, which is one of the most extensively used impingers, is now considered as the reference bioaerosol sampler, although impingers show low physical collection efficiencies for small particles like viruses. The physical collection efficiencies of viral aerosol particles of diameter 30–100 nm are lower than 50% (Hogan et al., 2005; Li et al., 2018). In addition, considering that long-term sampling deteriorates the collection efficiency of bacteria and exerts stress on the bacteria because of liquid loss and re-aerosolization during sampling (Chang and Chou, 2011; Rule et al., 2007; Zhen et al., 2013), similar effects can be assumed for airborne viruses as well.

4.2. Air sampler: cyclones

A cyclone usually comprises a conical-shaped body and tangentially installed flow inlet. Similar to the impactor, particles larger than the cut-off diameter deviate from the curved streamlines and impact with the collection wall. Conventional cyclones are mainly designed to collect large particles with high flow rates, and their collection efficiencies are slightly lower than those of impactors. For conventional single cyclones, which have air flow rates of the order of hundreds to more than thousands of LPM, the collection efficiency of PM10 (particulate matter with aerodynamic diameters less than 10 μm) is 30–90% and that of PM2.5 (particulate matter with aerodynamic diameters less than 2.5 μm) is 0–40% (Cooper and Alley, 1986); therefore, cyclone samplers alone may not be sufficient for collecting viral aerosols effectively.

The NIOSH developed a portable two-stage dry cyclone sampler with an embedded filter (Lindsley et al., 2006). The first and second stages of the sampler collected non-respirable particles larger than 4 μm and those between 1 and 4 μm, respectively; the PTFE filter in the third stage collected particles smaller than 1 μm, and the collected particles were eluted thereafter. The NIOSH cyclone (NIOSH-251) was used to collect airborne murine norovirus (MNV) and influenza viruses at 3.5 LPM (Bekking et al., 2019; Boles et al., 2020). It collected a significantly lower RNA concentration of the MNV than the SKC BioSampler; however, there were no significant differences in the relative concentrations of MNVs with intact capsids between the two samplers (Boles et al., 2020). Infectivity losses of influenza viruses were also observed during aerosolization and sampling (Bekking et al., 2019).

A wet cyclone collects aerosol particles onto a liquid film flowing along the interior wall; this device has been used to collect several airborne viruses, including influenza viruses at flow rates of about 100 LPM (Alonso et al., 2015) and foot-and-mouth disease virus (FMDV) at a

flow rate of 300 LPM (Brown et al., 2021). The FMDVs were nebulized at three concentrations (10^2, 10^4, and 10^6 $TCID_{50}$ mL^{-1}) but were not detected at a concentration of 10^2 $TCID_{50}$ mL^{-1}, implying that this sampler may not be effective for detecting small virus concentrations.

4.3. Air sampler: filter-based samplers

Generally, filtration is a common method of removing PM from air. Filters have the lowest removal efficiencies at particle diameters of 0.2–0.5 μm, and the physical collection efficiencies of most high-efficiency particulate air (HEPA) filters are usually greater than 95% for a wide range of particle sizes. Filters are convenient to use and can be used for air sampling; however, dehydration of filters during sampling and the extraction process affect their biological recovery significantly.

The most commonly used filter for sampling viral aerosols is the gelatin filter (Zhao et al., 2014; Li et al., 2018), which can be easily dissolved in a culture medium to allow gentle transition from gas to liquid phase after capturing the virus. However, gelatin filters have been recommended for sampling with short periods to prevent dehydration (Li et al., 2018; Fabian et al., 2009). Airborne infectious bursal disease viruses (diameter: 60–90 nm) were collected using MD8 with gelatin filters for 2 min at 30 LPM, where the physical collection efficiency was ~100% (Zhao et al., 2014). Sampling with a gelatin filter was reported to be stable for 3 min at 2 LPM, and higher flow-rate operations created large fluctuations in the physical collection efficiencies (Li et al., 2018). The SARS-CoV-2 virus was also collected using gelatin filters at 5 and 9 LPM for several hours or more, and qPCR was used for RNA quantification (Liu et al., 2020).

4.4. Air sampler: water-condensation-based samplers

Impactors and impingers are generally unable to collect viral aerosol particles effectively because of the small sizes. A water-based laminar-flow condensational growth tube collector (GTC, also called VIVAS or viable virus aerosol sampler) can enlarge the incoming small particles by passing them through a cold wall (called the conditioner) and a subsequent high-temperature wall (called the initiator) via water condensation to collect the resulting enlarged particles by impaction. The larger the temperature difference, the more is the condensation, which can increase the physical collection efficiency; however, high-temperature operation at the initiator can damage the viruses to be collected (Pan et al., 2016; Lin et al., 2018). These samplers were developed to collect

Table 4

Studies on the measurement of artificially generated viral aerosols. FFU: focus forming unit; PFU: plaque forming unit; FI: fluorescence intensity; LPM: liters per minute; qPCR: quantitative (real-time) polymerase chain reaction; qRT-PCR: quantitative reverse transcription-PCR; $TCID_{50}$: fifty-percent tissue culture infective dose; MMD: mass median diameter; PC: polycarbonates; PTFE: polytetrafluoroethylene; ESP: electrostatic precipitator; NW: nanowire; FET: field effect transistor; LOD: limit of detection; CMD: count median diameter; EID_{50}: fifty-percent egg infective dose; GTC: growth tube collector; TCI: Tisch cascade impactor; NIOSH: National Institute for Occupational Safety and Health; ROS: reactive oxygen species.

Sampler	References	Virus	Size	Flow rate (LPM)	Method	Result	Comments on viral damage
Impactor; Impinger; Filter	(Fabian et al., 2009)	Influenza virus (H1N1)	N/A	Impactor: 30; Impinger: 12.5; Teflon filter: 30; Gelatin filter: 30;	Plaque assay; qPCR	Infectiousness ($[qPCR/FFU]_{initial}$ /$[qPCR/FFU]_{collected}$) Impactor: 0.16–0.29; BioSampler: 0.75–1.10; Teflon filter: 0.15–0.43; Gelatin filter: 0.11–0.19	Liquid-based samplers preserved better virus infectivity than dry-media samplers.
Impactor	(Appert et al., 2012)	MS2 bacteriophages; Adenovirus	N/A	Andersen sampler: 28.3; MOUDI: 30	Plaque assay; Endpoint dilution assay	Relative recovery ($[Virus/FI]_{collected}$ /$[Virus/FI]_{initial}$) Andersen: 0.04–0.22; MOUDI: 0.02–0.1	
Impactor; Impinger; Cyclone; Filter; ESP	(Dybwad et al., 2014)	MS2 bacteriophages	MMD: 4 µm	BioCapture 650: 200; XMX-CV: 530; Coriolis FR: 300; SASS 2300: 390; SASS 3100: 300; Gelatin filter: 15; ESP: 540	PFU; qPCR	Relative efficiency ($PFU_{test\ sampler}$/$PFU_{BioSampler}$) BioCapture 650: 0.72; XMX-CV: 0.20; Coriolis FR: 0.70; SASS 2300: 0.64; SASS 3100: 0.01; Gelatin filter: 1.06; ESP: 0.03 Relative efficiency ($qPCR_{test\ sampler}$/$qPCR_{BioSampler}$) BioCapture 650: 0.69; XMX-CV: 0.16; Coriolis FR: 0.50; SASS 2300: 0.57; SASS 3100: 0.62; Gelatin filter: 0.22; ESP: 0.30	Dry-phase samplers decreased cultivability of MS2.
Impactor; Impinger; Filter	(Zhao et al., 2014)	Infectious bursal disease virus	1–10 µm (0 min); 1–5 µm (20 min)	Andersen sampler: 28.3; AGI-30: 12.5; OMNI-3000: 300; Gelatin filter: 30	Egg endpoint dilution assay	Biological efficiency ($[EID_{50}/FI]_{collected}$ /$[EID_{50}/FI]_{initial}$) Andersen sampler: 0.61 ± 0.30; AGI-30: 0.68 ± 0.25; OMNI-3000: 0.23 ± 10; Gelatin filter: 1	The tested virus seems to be more resistant to dehydration stress than shear stress.
Impactor	(Alonso et al., 2017)	Betaarterivirus suid 1; Influenza virus (H1N1)	N/A	Andersen sampler: 28.3; TCI: 1130	RT-PCR	Log_{10} RNA copies/m^3 (H1N1) Andersen Sampler: 5.7–6.3; TCI: 5.4–6.3 (PRRSV) Andersen Sampler: 7.8–8.2; TCI: 6.8–8	
Impinger; Filter	(Li et al., 2018)	Influenza virus (H1N1)	N/A	BioSampler: 12.5; Gelatin filter: 2–4; Glass fiber filter: 2–4	Endpoint dilution assay; qPCR	Relative recovery ($TCID50_{collected}$ /$TCID50_{initial}$) Biosampler: 0.001–0.01; Gelatin filter: < 0.00047; Glass fiber filter: < 0.00031	Extracting process from glass fiber filters may deactivate the viruses.
Cyclone	(Cao et al., 2011)	Influenza virus (H1N1)	CMD: 0.8 µm	Cyclone: 3.5; BioSampler: 12.5	Plaque assay; qPCR	Total viral particles per liter of sampled air Cyclone: 2.4×10^4; BioSampler: 2.6×10^4	Virus infectivity in the cyclone was 34% of that in the BioSampler.
Cyclone	(Boles et al., 2020)	Norovirus	N/A	NIOSH sampler: 3.5; BioSampler: 12.5	qPCR; PMA assay (propidium monoazide dye)	Airborne viral concentration (RNA copies/m^3) NIOSH: 1.16×10^4–1.66×10^4; BioSampler: 4.75×10^4 –8.78×10^4	
Filter	(Verreault et al., 2010)	Phi X 174 bacteriophages; Lactococcus virus P008	MMD (µm), Phi X 174: 1.3; Lactococcus virus P008: 1.7	2	Plaque assay; qPCR	Relative recovery ($qPCR_{collected}$ /$qPCR_{initial}$) (Phi X 174) PC filter: 0.06–0.15; PTFE filter: 0.02–0.04 (Lactococcus virus P008) PC filter: 0.3–1.7; PTFE filter: 0.3–1.4 Relative recovery	

Table 4 (*continued*)

Sampler	References	Virus	Size	Flow rate (LPM)	Method	Result	Comments on viral damage
						(PFU$_{collected}$/PFU$_{initial}$) (Phi X 174) PC filter: 0.00005–0.0002; PTFE filter: 0.00005–0.00015 (Lactococcus virus P008) PC filter: 0.00005–0.023; PTFE filter: 0.002–0.008	
Condensation	(Oh et al., 2010)	MS2 bacteriophages	N/A	12.5	Plaque assay	Factor multiplying collection efficiency (PFU$_{on}$/PFU$_{off}$) 1.08–2.22	The collection efficiency was highest for a saturated air temperature of 65 °C.
Condensation	(Pan et al., 2016)	MS2 bacteriophages	N/A	GTC: 7; BioSampler: 12.5	Plaque assay	Concentration in air (PFU/L) GTC: 1721; BioSampler: 12.4	Viable MS2 concentration decreased when initiator temperature increased to 60 °C.
Condensation	(Lednicky et al., 2016)	Influenza virus (H1N1)	Mode diameter: 2.6 μm	VIVAS: 6.86; BioSampler: 12.5	Endpoint dilution assay	Collection efficiency (TCID50$_{collected}$/ TCID50$_{nebulized}$) VIVAS: 0.74 ± 0.12; BioSampler: 0.056 ± 0.03	Collection efficiency decreased with the loss of virus viability during the collection process in the BioSampler.
Condensation	(Walls et al., 2016)	MS2 bacteriophages	Mode diameter: 35 nm	GTC: 7; AGI-4: 12.5	Plaque assay; qRT-PCR	Percent infectivity GTC: 0.044–0.054; AGI-4: 0.044–0.071	Percent infectivity increased as the particle diameter increased.
Condensation	(Jiang et al., 2016)	MS2 bacteriophages	N/A	GTC: 7; BioSampler: 12.5	Plaque assay	Collection efficiency (PFU$_{collected}$/PFU$_{nebulized}$) GTC: 0.0024–0.018; BioSampler: 0.00008	The collection efficiency increased with relative humidity.
Condensation	(Lin et al., 2018)	MS2 bacteriophages	N/A	12.5	Plaque assay	Viral aerosol collection enhancement factor (PFU$_{on}$/PFU$_{off}$) AGI-30: 1.69–6.69; BioSampler: 4.77–21.59	Viral aerosol collection enhancement factor decreased when mixing reservoir temperature increased to 50 °C.
ESP	(Shen et al., 2011a)	Influenza virus (H3N2)	N/A	5	Si-NW FET	Detection range (gene copies/μL) $1.8 \times 10^4 - 7 \times 10^7$	LOD of $< 10^4$ viruses per liter of air
ESP	(Hong et al., 2016)	MS2 &T3 bacteriophages	Mode: 36 nm	1.2–12.5	PFU; qPCR	Recovery rate ([PFU/qPCR]$_{collected}$/[PFU/qPCR]$_{initial}$) (MS2) ESP: 0.975 (−2 kV); BioSampler: 0.794 (T3) ESP: 0.666–0.943 (−2 kV); BioSampler: 0.001–1.12	The recovery rate decreased with sampling velocity in the BioSampler.
ESP	(Ladhani et al., 2017)	Influenza virus (H1N1 & H3N2)	MMD: 1.074 μm	6.8	qPCR	Collection efficiency (qPCR$_{ESP}$/qPCR$_{gelatin\ filter}$) 0.0424–0.47	Additional extraction process was required to obtain high collection efficiency.
ESP	(Bhardwaj et al., 2020)	Influenza virus (H1N1)	Mode: 36 nm	1.2	Electrochemical paper sensor	Detection limit (PFU/mL) 2.13	ROS in the ESP damaged hemagglutinin of the viruses.
ESP	(Kim et al., 2020b)	Human coronavirus 229E; Influenza virus (H1N1 & H3N2)	Mode diameter, Human coronavirus 229E: 109 nm; Influenza virus H1N1 & H3N2: 95 nm	4–10	qRT-PCR	Total enrichment capacities $2.4 \times 10^6 - 3.0 \times 10^6$	Higher aerosol-to-hydrosol enrichment capacities were obtained for lower aerosol concentrations.

small virus particles while maintaining viability because the enclosing water droplet enables gentle collection (Pan et al., 2016; Lednicky et al., 2016). However, its relatively low flow rate for condensation and bulkiness (considerable size and weight) are the current limitations (Pan et al., 2019). The GTC showed more than 10 times higher collection efficiency for the MS2 bacteriophages and 7 times higher collection efficiency for the influenza A viruses than the BioSampler (Pan et al., 2016; Lednicky et al., 2016); it has also been used to isolate several viable viruses, such as influenza viruses and coronaviruses (HCoV-229E) at a student healthcare center (Pan et al., 2017) and viable SARS-CoV-2 in a hospital room with patients (Lednicky et al., 2020).

Direct mixing of the particles with supersaturated water vapor can also increase the sizes of the aerosols. Oh et al. (2010) developed a mixing-type bioaerosol amplification unit (mBAU) to mix the incoming

aerosols with hot-water-saturated air, and the number of viable MS2 bacteriophages was reported to increase by 2–3 times after passing through the mBAU. Lin et al. (2018) developed a steam-jet aerosol collector (SJAC) for bioaerosol collection, where the incoming aerosols were mixed with hot steam to achieve supersaturated conditions and condensational growth. The SJAC combined with the BioSampler showed 22 times more viable MS2 bacteriophages than the BioSampler alone (Lin et al., 2018).

4.5. Air sampler: electrostatic samplers

In the ESP, airborne particles gain electrical charge via unipolar charging, and the charged particles migrate to an electrically biased collection surface via electrostatic forces. Since airborne particles

generally have natural charge distributions for each size with a median value of zero according to the Boltzmann distribution, it is difficult to efficiently collect them without artificial unipolar charging. In such cases, a corona discharger is commonly used and generates a large amount of unipolar (positive or negative) ions via a nonuniform electrostatic field.

Recently, studies on electrostatic samplers are being actively conducted because of their advantages such as high collection efficiency for particles of the order of submicron to tens of micrometers and ability to concentrate particles in a small amount of liquid (Bhardwaj et al., 2020; Hong et al., 2016; Kim et al., 2020b; Ladhani et al., 2017). Moreover, they show lower impaction stress on the bioaerosol particles and lower pressure drop. However, such samplers are still subject to some problems: ozone and ROS emissions, low collection efficiency at high flow rates and/or small collection areas, charger degradation during the sampling process, and difficulty in charging nanometer-sized particles. ROS emission is an important issue and can inactivate microorganisms collected on the electrostatic sampler (Bhardwaj et al., 2020; Zukeran et al., 2018). The U. S. Food and Drug Administration (FDA) requires that ozone emission should be lower than 50 parts per billion (Han et al., 2017). Moreover, high electric fields must be applied, and the charging conditions can vary depending on temperature and RH, thus making standardization difficult.

Dybwad et al. (2014) evaluated nine air samplers, including an ESP with a flow rate of 540 LPM, for sampling MS2 bacteriophages. The ESP showed a biological collection efficiency (based on PFU) of 0.03 and physical collection efficiency (based on qPCR) of 0.3 relative to the BioSampler. The low biological recovery was due to dry phase sampling in the ESP. Ladhani et al. (2017) developed an ESP for point-of-care applications and collected aerosolized submicron-sized influenza A viruses. The collection efficiency (based on qPCR) relative to a gelatin filter varied from 4.24% to 47% at a flow rate of 6.8 LPM. To increase the collection efficiency, additional wiping and rinsing processes were required to extract the viruses adhering to the collector surfaces. A portable electrostatic particle concentrator (EPC) was also presented for concentrating submicrometer MS2 and T3 bacteriophages in 0.5 mL phosphate buffered saline (PBS) on the small collection electrode at a flow rate of 1.2–12.5 LPM (Hong et al., 2016); its collection efficiencies based on the inlet and outlet concentrations were over 99% for 0.05–2 μm polystyrene particles at 1.2 LPM, and the MS2 and T3 concentrations were 10 times higher than those for the BioSampler. The viable concentration of the fragile T3 viruses was 982 times higher in the EPC than the BioSampler; this result was attributed to the significantly lower sampling velocity in the EPC. The EPC was further evaluated for sampling aerosolized submicron influenza A H1N1 virus particles and subsequent detection using an electrochemical paper-based sensor (Bhardwaj et al., 2020). It was found that high electric fields resulted in direct and indirect peroxidation of the lipids and hemagglutinin proteins on the viruses; however, the antigenicity of NPs of the viruses was preserved, and a 160 times higher virus concentration was obtained after 60 min of sampling compared to the BioSampler. Electrostatic virus collectors were also used to extract the RNAs of the coronavirus 229E and influenza viruses (H1N1 and H3N2) using PCR at 4–10 LPM (Kim et al., 2020b); these collectors were further developed to work at higher flow rates of up to 100 LPM and collection efficiencies of 70–80% at − 10 kV using a larger collection area (Kim et al., 2021). Ascorbic acid added into sampling media was observed to reduce virus damage caused by electrostatic sampling (Piri et al., 2021).

5. Virus measurements

5.1. Classification of measurements of viral aerosol particles

Viral aerosols are usually detected and/or measured using the growth method, nucleic-acid-based techniques, or immunoassays. The growth techniques can detect only viable viruses, but immunoassays can detect not only viable viruses but also non-viable viruses by identifying specific intact proteins. The choice of the measurement method depends strongly on the extent to which the viruses are damaged. In fact, environmental stress such as ambient temperature and humidity, ROS, and UV light, as well as aerosol generation and sampling can cause physical and biological damage to certain parts of the viruses, e.g., nucleic acids and surface/inner proteins, resulting in loss of viability (Christopher and GwangPyo, 2007; Bekking et al., 2019; Sagripanti and Lytle, 2020).

The measurement methods for viral aerosols are usually categorized according to the specific states of the viruses, such as plaque forming viruses, non-plaque forming infectious viruses (infectious viruses but fail to generate plaques sometimes), dead-but-intact viruses (cannot multiply but possess intact DNA/RNA or proteins), and dead-and-not-intact viruses (cannot multiply without intact DNA/RNA or proteins). Table 5 shows the classification for detection of viral aerosols, and Table 6 shows some studies on viral aerosols involving both samplers and measurement systems.

5.2. Plaque and fifty percent tissue culture infective dose (TCID$_{50}$) assays

The culture-based plaque and TCID$_{50}$ assays are gold standard and traditional methods for quantifying the concentration of infectious viruses (or infective dose). The plaque assay is a microbiological assay based on the viral plaques formed via the cytopathic effect, or morphological changes in host cells due to viral infection. The plaque assay first requires inoculation with an infectious virus, propagation, and then plaque counting. Visible plaques generally form within 2–14 days depending on the host cell and growth of the virus (Baer and Kehn-Hall, 2014), which makes the process time intensive. For bacteriophages, the process requires 12–24 h, but for some animal viruses, a longer time is required. The plaque assay can significantly underestimate the total concentration of the virus in air because there are only a small amount of viable viruses among the viruses in air and all viable viruses cannot generate plaques (Blais-Lecours et al., 2015). The TCID$_{50}$ assay is a widely used method to quantify the infectious dose of viruses required to kill 50% of inoculated tissue culture cells. This can be used for infectious virus that fails to generate plaques sometimes. In fact, it was reported that about 90% of influenza A viruses are capable of infecting cells or causing cell death but do not form plaques using traditional assays (Brooke, 2014).

5.3. Nucleic-acid-based amplification method

Nucleic-acid-amplification assays like PCR have been used in most studies on the measurement of airborne viruses because these viruses are subject to damage during transmission through the air and sampling, especially in inertial samplers, and exist in very small quantities. PCR is currently the gold-standard method for measuring viruses in clinical and air samples, and it is the most effective method for detecting low concentrations of viruses. PCR can detect 4–8 copies of the SARS-CoV-2 within a 95% confidence interval (Rahmani et al., 2020).

PCR detects and amplifies a particular DNA sequence from the collected viral samples and involves an initial denaturation, 20–40 cycles of denaturation, annealing, and extension (King et al., 2020). Reverse transcription PCR (RT-PCR) requires mRNA as the starting material and converts this mRNA into complementary DNA (cDNA) using reverse transcriptase (Mo et al., 2012). Then, the cDNA is amplified using conventional PCR. This process is complicated and time consuming for RNA viruses because it requires the additional step of cDNA template synthesis using RT-PCR (Bhardwaj et al., 2021). The qPCR is similar to conventional (qualitative) PCR but requires a nonspecific dye, such as SYBR® green dye, for real-time quantification of the dsDNA PCR product (Gupta, 2019). PMA-qPCR can also be used to differentiate between intact and membrane-compromised viruses using RNA/DNA intercalating propidium monoazide (PMA) dye, which can penetrate the viruses with damaged capsids (Bonifait et al., 2015).

Table 5

Classification of detection methods that can be used for viral aerosols. TCID$_{50}$: fifty-percent tissue culture infective dose, qPCR: quantitative polymerase chain reaction, ELISA: enzyme-linked immunosorbent assay, RIA: radio immunoassay, MALDI-TOF: matrix assisted laser desorption/ionization time-of-flight, ATP: adenosine triphosphate, PMA: propidium monoazide, QCM: quartz crystal microbalance, SPR: surface plasmon resonance, FET: field effects transistor, UVAPS: ultraviolet aerodynamic particle sizer, NADH: nicotinamide-adenine dinucleotide.

Detection method	Type of detection	Specific to state of virus	Limitation	Comments	References
Culturing techniques	Plaque TCID$_{50}$	Only plaque forming virus Both plaque forming and non-plaque forming infectious viruses	Specific culture conditions necessary; cannot be used for non-infectious viruses		(Brooke, 2014)
Molecular	qPCR, droplet digital PCR, Isothermal PCR techniques	Plaque forming, non-plaque forming, and dead viruses (with intact DNA/RNA)	Quantification may be highly affected by contamination, nucleic acid extraction and improper sampling; time consuming		(Kim et al., 2021; Sharma Ghimire et al., 2019)
	PMA-qPCR	Differentiate intact from compromised virions			(Bonifait et al., 2015)
Immunoassay (Chemical tracer/ Biochemical assay)	ELISA	Both plaque forming and non-plaque forming infectious virus.	Time consuming; knowledge about specific antibodies	No report on viral aerosols yet	(Ghosh et al., 2015b)
	RIA	Dead virus and specific protein of a virus	Specific chemical labeling		
	Neuraminidase (NA) activity	Both plaque forming and non-plaque forming infectious viruses	NA activities are present for several viruses including influenza A, B, parainfluenza, and rubella viruses. Environmental stresses affect NA activity.	A commercialized kit is for influenza viruses only.	(Turgeon et al., 2011)
Affinity based sensors	QCM, SPR, FET, Electrochemical sensors	Both plaque forming and non-plaque forming infectious viruses. Dead viruses with intact protein or RNA/DNA	Surface protein based affinity sensors can fail to detect when the surface proteins of target viruses are degraded or damaged.		(Bhardwaj et al., 2020)
Microscopy	Electron microscopy	Both plaque forming and non-plaque infectious forming viruses. Dead viruses (with and without intact DNA), cell fragments or proteins		No reports on viral aerosol detection	(Ghosh et al., 2015b, 2015c)
Fluorescence based quantitative analysis	Flow cytometry				(Lippe, 2018)
Mass spectrometry	MALDI-TOF	plaque forming and non-plaque forming infectious viruses, dead and fragments	Compounds less than 600 Da in size cannot be detected	No reports on viral aerosol detection	(Cardozo et al., 2020)
Optical	ATP bioluminescence	Cannot be used for any state of viruses	applicable to bacteria, fungi, and mycoplasma	This method is based on auto-fluorophores of bio-particles such as NADH etc., and metabolic activity markers such as ATP.	(Yoon et al., 2019; Su et al., 2020)
	UVAPS	Cannot be used for virus detection	Only applicable to viable bacteria & fungi		

PCR is highly sensitive and can distinguish targets at the species level, but it requires a time-consuming nucleic-acid extraction process that may require up to 2–3 h for detection, in addition to the sampling time (< 30–60 min), cannot distinguish between infectious and non-infectious viruses, and is susceptible to sample contamination and RNA/DNA losses, which can underestimate the actual viral concentration (Xu et al., 2011). Another limitation of PCR amplification is that the samples can contain compounds, such as humic acid, high concentrations of non-target DNA, and organic compounds (Oppliger et al., 2011; Schrader et al., 2012) that are typically present in air samples and can hinder PCR amplification. Hence, intervention by PCR inhibitors should be evaluated before using PCR for air samples. For example, ethylenediaminetetraacetic acid (EDTA), which may be present in the substrate cleaning solutions of impactors, inhibits PCR amplification; therefore, the concentration of EDTA should be reduced before PCR amplification (King et al., 2020).

A few studies have attempted an integrated detection system with air samplers for rapid on-site detection. Usachev and Agranovski (Usachev and Agranovski, 2012) detected T4 bacteriophages using personal air samplers integrated with qPCR by loading all the reagents into collection media before qPCR without need for RNA purification. The total measurement time including sampling was 70 min (sampling: 10 min and qPCR: 1 h), and the LOD was 24 PFUs per reaction. Agranovski et al. (2017) developed a miniature real-time PCR-based portable bioaerosol monitoring system; this system can detect within 30–80 min on-site for aerosol particles larger than 0.2 μm, and the PCR analysis commenced after certain abnormal signals were observed. Kim et al. (2020b) developed an integrated system of electrostatic sampling and qPCR detection, which was used for detection of airborne coronaviruses and

influenza viruses along with high viral enrichment.

Several isothermal nucleic-acid-based assays, such as the simple amplification-based assay (SAMBA), loop-mediated isothermal amplification (LAMP) assay, and nucleic acid sequence-based amplification (NASBA), have been developed to improve the sensitivity and decrease the assay time and cost of conventional RT-PCR (Fig. 7). LAMP is one of the most commonly used isothermal techniques because it can be performed without a commercial thermocycler in less time (~30 min), and it can be integrated with different (colorimetric, luminometric and fluorescent) readouts (Khan et al., 2020). RT-LAMP (for RNA viruses) based portable system was used for detection of SARS-CoV-2 in clinical samples using a cartridge and smartphone based optical reader without any extra equipment for sample preparation, mixing, and amplification (Ganguli et al., 2020). However, very few studies have considered integration with air samplers (Agranovski et al., 2017; Usachev et al., 2012). Recently, a three-dimensional paper-based RT-LAMP method was used for detection of airborne influenza H1N1 viruses using VIVAS (Jiang et al., 2021). This integrated device detected the viruses in 50 min after 15 min sampling, and the LOD was 1 TCID$_{50}$/140 μL. The collection paper pad was removed from VIVAS after sampling for RNA enrichment and amplification via RT-LAMP.

5.4. Immunoassay

Immunological assays are based on the binding of (polyclonal or monoclonal) antibodies specific to their target analytes (surface proteins and/or polysaccharides) and can be used for detection of bioaerosols. Immunoassays such as ELISA and radioimmunoassay (RIA) have been used for rapid, selective, and sensitive quantification of viruses in

Table 6

Conventional and advanced methods for detection of viral aerosols. UTM: universal transport medium, NIOSH: National Institute for Occupational Safety and Health, G-II: Gesundheit-II, qPCR: quantitative polymerase chain reaction, ddPCR: droplet digital polymerase chain reaction, PFU: plaque forming units, NP swabs: naso-pharyngeal swab, PBS: phosphate buffered saline, VTM: viral transport medium, HBSS: Hanks balanced salt solution, VIVAS: viable virus aerosol sampler, AAB: ammonium acetate buffer, DI: deionized water, TYB: tryptone yeast extract broth, BSA: bovine serum albumin, TCID50: 50% tissue culture infectious dose, EID$_{50}$: 50% egg infectious dose, GTC: growth tube collector, PMA: propidium monoazide, UNMC: University of Nebraska Medical Center, AIIR: airborne infection isolation rooms, LAMP: loop-mediated isothermal amplification, SiNw: silicon nanowire, swCNT: sigle-walled carbon nanotube, EAD: electro aerodynamic, EBC: exhaled breath condensate.

Detection method	Sampler	Target	Locations	Collection liquid	Detection limit	References
Growth, ELISA, and nucleic-acid-based methods						
qPCR	NIOSH-2	Influenza A virus	Virginia University Hospital	Lysis and binding solution		(Blachere et al., 2009)
qPCR, Culture (Plaque assay)	NIOSH-2	Influenza A virus	nasal swab and cough samples	UTM	qPCR= 83 copies/cough Plaque assay= 0.8 PFU/cough	(Lindsley et al., 2010)
qPCR, Culture (Plaque assay)	G-II human source sampler	Influenza A virus	Exhaled breath	PBS+ 0.01% BSA	Plaque assay= 3.0×10^5 qPCR= 1.8×10^8 copy number	(McDevitt et al., 2013)
qPCR, Culture (Plaque assay)	G-II human source sampler	Influenza A virus	Breath, talk, cough, and sneeze	PBS+ 0.01% BSA	Plaque=fine aerosol (39%) & -NP swabs (89%) qPCR= fine aerosol (3.8×10^4 copies), NP swabs (8.2×10^8 copies)	(Yan et al., 2018)
Culture assay (TCID50)	VIVAS	Influenza A virus (H1N1)		PBS+ 0.5% BSA		(Lednicky et al., 2016)
Culture (Plaque assay), ELISA	VIVAS	Influenza A virus (H1N1 H3N2), Influenza B virus	Air samples at health care center	PBS+ 0.5% BSA		(Pan et al., 2017)
Culture (Plaque assay)	GTC	MS2		1.5 mL of DI water or TYB	DI= 442 ± 305 PFU/ L TYB= 1721 ± 335 PFU/L	(Pan et al., 2016)
Culture (Plaque assay), qPCR	NIOSH-2	Norovirus	Healthcare facilities of Quebec City	PBS		(Bonifait et al., 2015)
RT-PCR	Personal Cascade Impactor Sampler	Influenza A virus (H3N2)	apartment	PBS with 0.5% w/v BSA		(Lednicky and Loeb, 2013)
PMA-qPCR	SKC BioSampler and NIOSH-251	Murine norovirus (surrogate virus)	Laboratory (artificially generated)	PBS and HBSS	SKC BioSampler- 8.78×10^4 (HBSS) and 4.75×10^4 RNA copies/m^3 (PBS) NIOSH-251 = 1.66×10^4 (HBSS) and 1.16×10^4 RNA copies/m^3 (PBS)	(Boles et al., 2020)
ddPCR	Cascade impactor and Filters	SARS-CoV-2	Hospital indoors (Wuhan)	Filters dissolved in DI water	Peak RNA concentration in the protective-apparel removal room (copies/m^3), 0.25–0.5 μm: 40; 0.5–1.0 μm: 9; > 2.5 μm: 7	(Liu et al., 2020)
Real time RT-PCR, Culture assay (TCID50)	Sartorius Airport MD8 air sampler with gelatin filter 80 mm)	SARS-CoV-2	UNMC (Patient's room)	PBS	0–1.75 copies/μL or 2.86 copies/ L of air	(Santarpia et al., 2020)
Real time RT-PCR	Sartorius MD8 air scan with gelatin filter (80 mm, 3 μm pore size)	SARS-CoV-2	Air sample-AIIRs, Sneezing, Spitting, Saliva	VTM	AIIR-9.2×10^2 copies/mL, Sneeze-2.54×10^4 copies/mL Spitting- 1.9×10^4 to 2.3×10^7Saliva-3.30×10^6 and 9.17×10^7 copies/mL	(Chan et al., 2020)
Real time RT-PCR	ESP	Human coronavirus 229E; Influenza A virus (H1N1, H3N2)	Laboratory (artificially generated)	DI-water, PBS	Enrichment method -Con-A coated magnetic beads Liquid-0.08 PFU/mL, Air-1.2 PFU/m^3 time = <10 min	(Kim et al., 2020b)
Paper based RT-LAMP	VIVAS	Influenza A H1N1	Laboratory (artificially generated)	PBS+ 0.5% BSA	1TCID$_{50}$/140 μL	(Jiang et al., 2021)
Biosensors						
FET-immunosensor (SiNw)	Electrostatic sampler	Influenza A virus (H3N2)	Laboratory (stock virus)	DI water	10^4 virus μL^{-1}	(Shen et al., 2011b)
FET- immunosensor (SiNw)	BioStage impactor (SKC)	Influenza A virus (H3N2)	Laboratory-EBC	DI water	29 viruses μL^{-1}	(Shen et al., 2012)
FET-immunosensor (swCNT)	EAD	Influenza A virus (H1N1) and MS2	Laboratory-(stock virus)	PBS	–	(Park et al., 2015)
QCM immunosensor		Influenza A virus (H3N2)	Laboratory-(stock virus)		4 viruses mL^{-1}	(Owen et al., 2007)
QCM sensor	Impactor	Vaccinia virus	Laboratory- (stock virus)		40 particles /mL at a flow rate of 2.0 l/min	(Lee et al., 2008)
Near infrared (NIR) based LFA (Sandwich immunoassay)	Filter-based air sampler	MS2, Influenza A (H1N1)	Laboratory-(stock virus)	PBS	10^3 EID$_{50}$/mL (for H1N1) 10^6 PFU/mL (for MS2)	(Lee et al., 2020)
				PBS	2.13 PFU/mL for NP Ab	

Table 6 (*continued*)

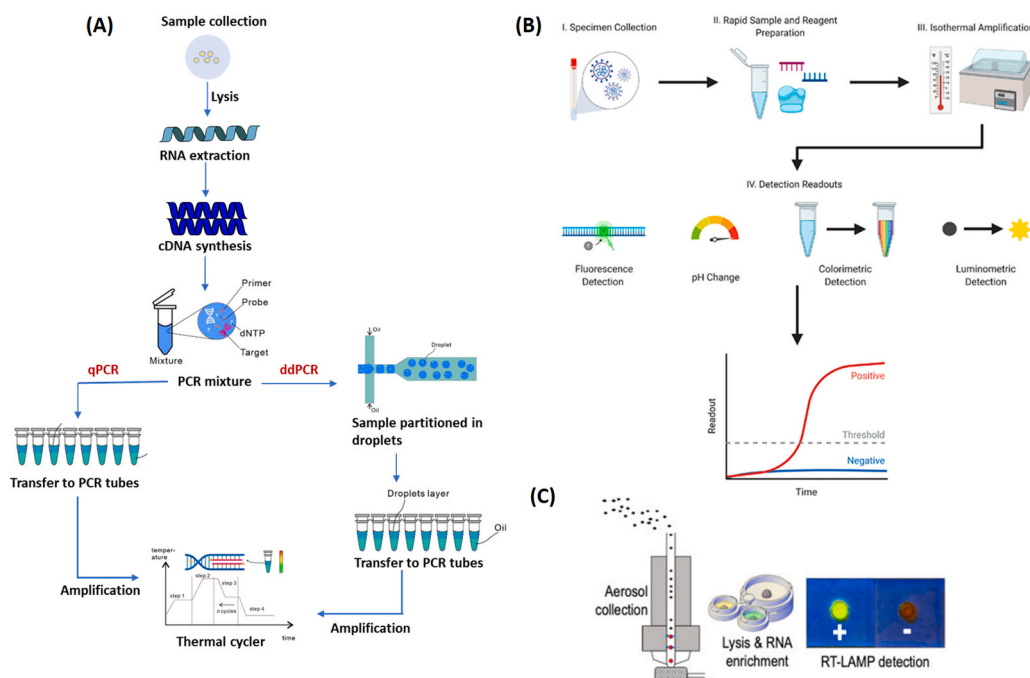| Detection method	Sampler	Target	Locations	Collection liquid	Detection limit	References
Electrochemical immunosensor (Paper-sandwich assay)	Electrostatic sampler (EPC)	Influenza A virus (H1N1)	Laboratory-(stock virus)			(Bhardwaj et al., 2020)

Fig. 7. (A) Schematics of qPCR and droplet digital PCR (image modified from Tan et al. (2021)), (B) workflow of the isothermal amplification process (image taken from Khan et al. (2020) with permission, © 2020 American Chemical Society), and (C) paper-based isothermal amplification technique (RT-LAMP) integrated with VIVAS for collection and detection of airborne influenza A H1N1 viruses (image taken from Jiang et al. (2021)).

clinical samples. Neuraminidase (NA) assay is an enzyme-based fluorometric assay for measuring NA activity, and it was used for clinical samples infected with influenza viruses (Turgeon et al., 2011). However, there have been no reports on viral aerosol detection using commercial immunoassays. This is partly because many of these techniques, especially ELISA, require lengthy analysis durations owing to multiple washing and incubation steps and separate imaging techniques after

sample capture (Fronczek and Yoon, 2015).

5.5. Affinity-based advanced viral aerosol measurement techniques

To date, several types of advanced platforms have been developed for measurement of viral aerosols, such as quartz crystal microbalances (QCMs), nanowire or carbon nanotube field effects transistors (FETs),
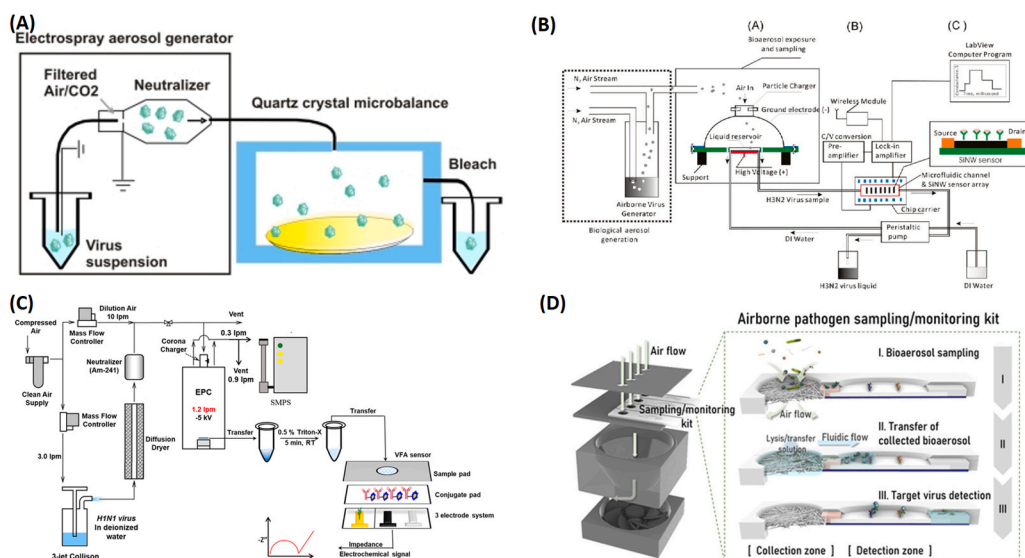

Fig. 8. Integrated sensor system with air samplers for detection of airborne viruses; (A) real-time quartz crystal microbalance sensor for detection of vaccinia viruses (image taken from Lee et al. (2008) with permission © 2008 American Institute of Physics Publishing LLC), (B) automated microfluidic nanowire-based FET immunosensor for detection of influenza A H3N2 viruses (image taken from Shen et al. (2011a)), (C) vertical flow assay (VFA)-based electrochemical paper immunosensor integrated with an electrostatic particle concentrator (EPC) for detection of influenza A H1N1 viruses (image taken from Bhardwaj et al. (2020)), and (D) lateral flow assay (LFA)-based optical immunosensor for detection of airborne influenza A H1N1 viruses and MS2 bacteriophages (image taken from (Lee et al. (2020)).

surface plasmon resonance (SPR), fluorescence-based technologies, and electrochemical biosensors, all of which can be manufactured in macroscale, microscale, or within microfluidic platforms (Fig. 8). Until now, most of these techniques have not been fully applied for field detection owing to experimental difficulties in working with real bio-aerosols, such as low concentrations of the viral aerosols as well as potential virus damage during the sampling process.

The QCM detects the presence of analytes via shifts in the resonant frequency of a quartz crystal when the analyte attaches to it and finds the mass based on the relationship between the additional mass and frequency shift. This technique has gained much attention because of the simple and real-time detection. Owen et al. (2007) developed the first antibody-functionalized QCM sensor for detection of viral aerosols (influenza virus H3N2), where the sampling method was not fully characterized. Airborne vaccinia viruses were also detected using a real-time gas-phase QCM sensor with a minimum detectable concentration of 40 and 210 virus particles per 1 mL of the virus suspension, which was prepared for aerosol generation, at flow rates of 2.0 and 1.1 LPM, respectively; however, selective detection was not provided because the QCM sensor did not involve bio-recognition elements on the surface (Lee et al., 2008).

Microfluidic platforms have been recently used for bioaerosol detection for serial processes of air sampling, waterborne sample transport, and bioassay to enhance detection sensitivity, to obtain rapid assays, and for continuous monitoring, etc. (Huffman et al., 2019). However, no microfluidic devices are commercially available for bio-aerosols until now despite the potential and laboratory-level demonstrations of microfluidic-coupled bioaerosol detection (King et al., 2020; Huffman et al., 2019). Moreover, the integration of nanosensors with microfluidic technologies is a promising approach for bioaerosol measurements; however, it is not easy to guide and capture the target analytes on a small detection area, and the stability and lifetime of an antibody-based nanosensor can deteriorate when exposed to environmental conditions (Xu et al., 2011).

A label-free FET nanowire sensor can be used to measure biological particles in liquid samples, where a change in the conductance of the nanowire is observed after binding of the target viruses to the antibody-functionalized channel of the FET. A nearly automated microfluidic FET device with antibody-coated silicon nanowires was developed for detection of airborne influenza viruses (H3N2) that were captured with an ESP (Shen et al., 2011a). The detection time of the FET device was 2 min, but this system was not fully automated (required manual handling) and the LOD was high ($\sim10^7$ viruses/mL for liquid-borne H3N2 viruses); it was also used for detection of influenza H1N1 viruses in clinical exhaled-breath-condensate samples with a detection limit of 29,000 viruses/mL (Shen et al., 2012).

The SPR method optically detects changes in the refractive index on the sensor surface when the analytes are bound to specific bioreceptors immobilized on the sensor surfaces and can provide real-time detection of the target analytes (proteins, small organics, microbes, viruses, or toxins). This sensor is generally fabricated using a thin gold coating on a glass substrate. Usachev et al. (2013) developed an SPR system for detecting airborne MS2 viruses along with three bubbler-type samplers, and the total time (sampling and measurement) for analysis was 6 min; they further developed a multiplexed SPR sensor for detecting viral aerosols (MS2 and influenza A virus), and the LODs were 6×10^6 PFU and 7×10^5 PFU/mL for liquid viral samples of MS2 and influenza A viruses, respectively (Usachev et al., 2015, 2014). However, these systems can detect only high concentrations of airborne viruses.

Kwon et al. (2014) presented another optical (Mie scattering) assay using a smartphone camera to measure through microfluidic channels; here, the influenza A viruses (H1N1/2009) were bound with antibody-conjugated latex beads for size increase. Airborne viruses were collected with a button air sampler (or filters) and were transferred to an immunoassay-based microfluidic device. This optical measurement was rapid ($\sim$5 min) and sensitive, with an LOD of 10 pg ($\sim2 \times 10^4$

viruses)/mL for the sample solution.

The electrochemical biosensor is a device that produces measurable electrochemical signals proportional to the concentrations of antigens. These sensors usually contain an electrochemical cell employing three electrodes: a working electrode, a counter electrode, and a reference electrode. When a voltage is applied across the electrodes, electrochemical reactions occur in the presence of a redox mediator, which produces a change in the current through or resistance across the electrode proportional to the antigen concentration. The electrochemical detection method has been used for measurement of waterborne influenza viruses in clinical samples owing to its sensitive, low-cost, and rapid analysis compared to conventional techniques (Dziąbowska et al., 2018). The results are promising and may be applicable for detection of airborne viruses as well. Bhardwaj et al. (2020) presented the first study on the detection of airborne influenza viruses using paper-based electrochemical immunosensors following electrostatic sampling. These paper sensors could detect the amount of surface-protein-damaged viruses and all the collected viruses via hemagglutinin antibody (HA-Abs) and nucleoprotein antibody (NP-Ab) functionalization on the sensors, respectively. The measurements of the NP-Ab-based sensors were as good as those of qPCR, with an LOD of 2.13 PFU/mL. Lee et al. (2020) developed a lateral flow assay (LFA)-based paper sensor for collecting and detecting airborne viruses. After virus capture on the sample pad, loading buffer was injected on the pad, the collected viruses were moved to the detection zone, and signals were measured within 20 min using a portable NIR (near infrared) signal reader. This portable integrated system could be applied for on-site detection of airborne viruses.

5.6. Optical detection and viral vs. bacterial detection

Optical detection of bioaerosols has garnered much attention because of the noninvasive and real-time detection capabilities, but most of these techniques are limited to non-viral aerosols because of the small sizes of the viruses. Here, several optical detection techniques, such as fluorescence and adenosine triphosphate (ATP) monitoring, mass spectrometry (MS), and Raman spectroscopy (RS), are introduced along with their limitations for viral aerosol measurements.

Fluorescence detection is one of the most common optical detection methods based on pathogen-induced fluorescence. The fluorescence techniques include flow cytometry and laser-induced fluorescence (LIF), such as that using an ultraviolet aerodynamic particle sizer (UVAPS), both of which are generally used for detection of bacteria rather than viruses because of the very small signals obtained from viruses.

Flow cytometry requires labeling in liquids with nucleic-acid-binding fluorescent dyes (e.g. propidium iodide) or probes, that is, specific antibodies for the proteins to differentiate biological from non-biological particles (e.g. dust particles). A new version of flow cytometry was introduced as flow virometry for detection of small viruses because the normal detection range of flow cytometry is 300–500 nm (Lippe, 2018). Till date, there is no study on detection of viral aerosols, and the reason for this might be the time-consuming procedure of sample preparation (labeling and fixation etc.) for flow virometry (Bonar and Tilton, 2017).

LIF is based on the fluorescent intensities of the auto-fluorophores present in bacteria, fungi, and viruses. The common auto-fluorophores present in bioaerosols are nicotinamide-adenine dinucleotide (NADH) (a coenzyme), riboflavin, and amino acids (tryptophan and tyrosine), all of which have different excitation and emission wavelength ranges. These amino acids have 260–280 nm and 280–360 nm, while NADH has 340–360 nm and 440–470 nm, and riboflavin has 450–488 nm and 520–560 nm ranges for excitation and emission, respectively. Viruses contain small amounts of auto-fluorophores (tryptophan and tyrosine) that do not fluoresce by 405 nm light, while the main sources of fluorescence, NADH and riboflavin, are absent in individual viruses (Hill et al., 2013). Therefore, auto-fluorophore-based detection methods are not suitable for detection of airborne virus particles (Yoon et al., 2019).

UVAPS, one of the most well-known equipment using LIF, is used for real-time detection of viable bioaerosols by measuring the fluorescence signals in the size range of 0.5–15 μm using ultraviolet (UV) laser excitation at 355 nm and emission in the range of 420–575 nm (Xu et al., 2011; Uk Lee et al., 2010). Although UVAPS is a promising device, it cannot differentiate at the species level and has limitations for measuring viruses, bacterial spores, and dead bioaerosols (Xu et al., 2011; Lee et al., 2010). More details on these techniques are reviewed in (Huffman et al., 2019).

Another optical detection method uses ATP bioluminescence. This method monitors the microbial metabolisms, unlike other immunoassays and molecular approaches. Till date, this technique has been used for bacterial and fungal samples alone, and there are no reports on detection of viral aerosols because of the absence of ATP in viruses (Su et al., 2020).

MS is a laser-based approach that measures the molecular mass and electrical charges, or the mass-to-charge ratios, of biomolecules, including proteins and nucleic acids, from ionized samples followed by comparison with a database of species profiles. Several variants of MS, such as aerosol time-of-flight mass spectrometry, atomic mass spectrometry, and matrix-assisted laser desorption/ionization time-of-flight (MALDI-TOF) have been discussed in previous reviews (Ghosh et al., 2015a). Although MALDI-TOF was used in the molecular diagnostics of viral infections (Ganova-Raeva and Khudyakov, 2013) and detection of SARS-CoV-2 (Cardozo et al., 2020) in clinical samples, it is not appropriate for rapid detection of viral aerosols because it requires an enrichment step, such as PCR or cell culture, to prepare highly concentrated samples. For instance, respiratory disease viruses were grown and concentrated via ultra-centrifugation before extracting viral proteins (Calderaro et al., 2016). Moreover, there are small quantities of viral proteins in viruses, and the molecular weights of viral proteins are high (>20 kDa) in contrast with the range used for standard microbiological diagnoses (2–20 kDa) (Milewska et al., 2020).

RS is a non-destructive vibrational technique that has been used for characterizing aerosol particles, and it is generally used for large-sized aerosol particles (larger than 1 μm) (Tirella et al., 2018). Surface-enhanced Raman spectroscopy (SERS) has gained much attention because it can overcome the size problems associated with normal RS (Sharma Ghimire et al., 2019). SERS has been applied for the detection of airborne bacteria using air samplers (Sengupta et al., 2005, 2007) and viruses in clinical samples (Chen et al., 2020); however, there are no reports on the detection of airborne viruses. More details on RS are reviewed in Chen et al. (2020).

6. Conclusion and future prospect

Rapid on-site measurement of airborne viruses is highly required to prevent the spread of air-transmissible diseases at early stages. Airborne virus measurement typically consists of two processes: air sampling and virus measurement. Therefore, reliable sampling of airborne viruses along with advanced measurement techniques is critical to effectively measure airborne viruses. To date, many sampling devices and techniques have been presented. However, a portable sampler that meets all the requirements of large flowrate sampling, biologically safe virus collection, high ER, and high collection efficiency for particles ranging from tens of nanometers to tens of micrometers in size remains a challenge; hence, only a limited information about airborne viruses is known. Recently, many techniques have been proposed to compensate for the problems of each sampler. For example, when collecting airborne viruses electrostatically, the ROS adversely affecting the viability and rapid detection capability of airborne viruses was reduced by adding ascorbic acid into a sampling medium (Bhardwaj et al., 2020; Piri et al., 2021). Furthermore, since the number of viruses in the air is very small, and there exist many non-target particles such as particulate matter, collected viruses should be purified and/or enriched prior to measurement to reduce false measurements.

From the standpoint of airborne virus measurement, a portable and sensitive real-time measurement system providing species-level specificity can be ideal, but there exist many technical limitations. Therefore, rapid (less than 1–2 h including sampling) unmanned measurement systems that can provide measurement data daily or twice a day are more reasonable and realistic for long-term monitoring purposes, unless viral aerosols of interest require immediate steps or the viral aerosol concentrations vary drastically. Moreover, these monitoring systems suggest that low-cost sensors should be used since long-term measurement may need a great many analytes and analysis time.

Currently, most airborne virus measurements are conducted by PCR due to the shortcomings of conventional air samplers. Although PCR has the advantage of being accurate, it usually requires expensive instruments, long processing times (several hours), and highly trained personnel for RNA/DNA purification and PCR setup. The isothermal nucleic acids amplification technology has emerged because it can provide more rapid detection with high sensitivity. Several reports have been published on rapid detection of SARS-CoV-2 in clinical samples using the isothermal techniques such as RT-LAMP and rolling circle amplification (RCA) (Oishee et al., 2021). RCA was integrated with electrochemical biosensors for rapid (< 2 h) detection of SARS-CoV-2 in clinical samples with an LOD of 1 copy/μL (Chaibun et al., 2021). Since conventional PCR requires high temperature that can be adverse for the sensing surfaces, isothermal amplification would be preferred over RT-PCR when combing with other sensing (colorimetric, electrochemical) techniques (Gupta et al., 2021); nevertheless, there are few reports on the detection of airborne viruses to date. Digital PCR (dPCR) is another emerging technology, which allows absolute quantification of viral RNA with higher sensitivity, precision, and stability than conventional qPCR, and is classified into droplet dPCR (ddPCR), chip-based dPCR, and microfluidic-based dPCR (Tan et al., 2021). ddPCR was used for the detection of SARS-CoV-2 in surface samples, where the samples were found positive by dPCR, but RT-qPCR failed to detect (Lv et al., 2020).

Affinity (antibody, aptamer, peptides etc.)-based biosensors can be used as alternatives to conventional PCR for rapid and long-term measurement of airborne viruses. They can meet the requirements of specificity, sensitivity, rapidity, portability, low cost, and ease of use. Especially, paper-based analytical devices such as VFA (Bhardwaj et al., 2020) and LFA (Lee et al., 2020) integrated with air samplers can be used as an inexpensive portable platform for monitoring airborne viruses because of their low cost, porous structure, high surface-to-volume ratios, portability, and capillary action. Nanomaterials such as carbon nanotubes and graphene are highly desirable to be incorporated in these sensors for enhancing the sensitivity of biosensors, and stable and reproducible film deposition would be critical for long-term monitoring systems (Bhardwaj et al., 2021). These nanomaterials demonstrate high surface-to-volume ratios and high electron transfer characteristics, which may be ideal for electrical and electrochemical biosensors. Aptamers and peptides are promising candidates for the recognition elements of the airborne virus measurement systems because of their low cost, ease of manufacturing, and less sensitivity to environmentally harsh conditions compared to conventional antibodies.

Selecting compatible sampling and detection methods is critical for obtaining reliable measurements. This selection is also critical for assessing the performance of viral aerosol inactivation equipment because damaged parts of airborne viruses can vary depending on inactivation techniques. Further development and improvement of effective sampling technologies and rapid measurement of viral aerosols will continue to remain open to new opportunities.

Declaration of Competing Interest

The authors declare that they have no known competing financial interests or personal relationships that could have appeared to influence the work reported in this paper.

Acknowledgments

References

Agranovski, I.E., Usachev, E.V., Agranovski, E., Usacheva, O.V., 2017. Miniature PCR based portable bioaerosol monitor development. J. Appl. Microbiol. 122, 129–138. https://doi.org/10.1111/jam.13318.

Alidjinou, E.K., Sane, F., Firquet, S., Lobert, P.E., Hober, D., 2019. Resistance of enteric viruses on fomites. Intervirology. https://doi.org/10.1159/000448807.

Alonso, C., Olson, B.A., Goyal, S., Raynor, P.C., Davies, P.R., Torremorell, M., 2017. Comparison of two size-differentiating air samplers for detecting airborne swine viruses under experimental conditions. Aerosol Sci. Technol. 51, 198–205. https://doi.org/10.1080/02786826.2016.1249278.

Alonso, C., Raynor, P.C., Davies, P.R., Torremorell, M., Núñez, A., Clifford, D., 2015. Concentration, size distribution, and infectivity of airborne particles carrying swine viruses. PLoS One 10, 0135675. https://doi.org/10.1371/journal.pone.0135675.

Appert, J., Raynor, P.C., Abin, M., Chander, Y., Guarino, H., Goyal, S.M., Zuo, Z., Ge, S., Kuehn, T.H., 2012. Influence of suspending liquid, impactor type, and substrate on size-selective sampling of MS2 and adenovirus aerosols. Aerosol Sci. Technol. 46, 249–257. https://doi.org/10.1080/02786826.2011.619224.

Baer, A., Kehn-Hall, K., 2014. Viral concentration determination through plaque assays: using traditional and novel overlay systems. J. Vis. Exp. 52065. https://doi.org/10.3791/52065.

Bekking, C., Yip, L., Groulx, N., Doggett, N., Finn, M., Mubareka, S., 2019. Evaluation of bioaerosol samplers for the detection and quantification of influenza virus from artificial aerosols and influenza virus–infected ferrets, Influenza Other Respi. Viruses. https://doi.org/10.1111/irv.12678.

Bender, A., Bui, L.K., Feldman, M.A., Larsson, M., Bhardwaj, N., 1995. Inactivated influenza virus, when presented on dendritic cells, elicits human CD8+ cytolytic T cell responses. J. Exp. Med. 182, 1663–1671. https://doi.org/10.1084/jem.182.6.1663.

Bhardwaj, S.K., Bhardwaj, N., Kumar, V., Bhatt, D., Azzouz, A., Bhaumik, J., Kim, K.H., Deep, A., 2021. Recent progress in nanomaterial-based sensing of airborne viral and bacterial pathogens. Environ. Int. 146, 106183 https://doi.org/10.1016/j.envint.2020.106183.

Bhardwaj, J., Kim, M.W., Jang, J., 2020. Rapid airborne influenza virus quantification using an antibody-based electrochemical paper sensor and electrostatic particle concentrator. Environ. Sci. Technol. 54, 10700–10712. https://doi.org/10.1021/acs.est.0c00441.

Binder, R.A., Alarja, N.A., Robie, E.R., Kochek, K.E., Xiu, L., Rocha-Melogno, L., Abdelgadir, A., Goli, S.V., Farrell, A.S., Coleman, K.K., Turner, A.L., Lautredou, C.C., Lednicky, J.A., Lee, M.J., Polage, C.R., Simmons, R.A., Deshusses, M.A., Anderson, B. D., Gray, G.C., 2020. Environmental and aerosolized severe acute respiratory syndrome coronavirus 2 among hospitalized coronavirus disease 2019 patients. J. Infect. Dis. 222, 1798–1806. https://doi.org/10.1093/infdis/jiaa575.

Blachere, F.M., Lindsley, W.G., Pearce, T.A., Anderson, S.E., Fisher, M., Khakoo, R., Meade, B.J., Lander, O., Davis, S., Thewlis, R.E., Celik, I., Chen, B.T., Beezhold, D.H., 2009. Measurement of airborne influenza virus in a hospital emergency department. Clin. Infect. Dis. 48, 438–440. https://doi.org/10.1086/596478.

Blais-Lecours, P., Perrott, P., Duchaine, C., 2015. Non-culturable bioaerosols in indoor settings: impact on health and molecular approaches for detection. Atmos. Environ. 110, 45–53. https://doi.org/10.1016/J.ATMOSENV.2015.03.039.

Boles, C., Brown, G., Park, J.H., Nonnenmann, M., 2020. The optimization of methods for the collection of aerosolized murine norovirus. Food Environ. Virol. 12, 199–208. https://doi.org/10.1007/s12560-020-09430-4.

Bonar, M.M., Tilton, J.C., 2017. High sensitivity detection and sorting of infectious human immunodeficiency virus (HIV-1) particles by flow virometry. Virology 505, 80–90. https://doi.org/10.1016/j.virol.2017.02.016.

Bonifait, L., Charlebois, R., Vimont, A., Turgeon, N., Veillette, M., Longtin, Y., Jean, J., Duchaine, C., 2015. Detection and quantification of airborne norovirus during outbreaks in healthcare facilities. Clin. Infect. Dis. 61, 299–304. https://doi.org/10.1093/cid/civ321.

Božič, A., Kanduč, M., 2021. Relative humidity in droplet and airborne transmission of disease. J. Biol. Phys. 47, 1–29. https://doi.org/10.1007/s10867-020-09562-5.

Brooke, C.B., 2014. Biological activities of 'noninfectious' influenza A virus particles. Future Virol. 9, 41–51. https://doi.org/10.2217/fvl.13.118.

Brown, J.S., Gordon, T., Price, O., Asgharian, B., 2013. Thoracic and respirable particle definitions for human health risk assessment. Part. Fibre Toxicol. 10, 12. https://doi.org/10.1186/1743-8977-10-12.

Brown, E., Nelson, N., Gubbins, S., Colenutt, C., 2021. Environmental and air sampling are efficient methods for the detection and quantification of foot-and-mouth disease virus. J. Virol. Methods 287, 113988. https://doi.org/10.1016/j.jviromet.2020.113988.

Calderaro, A., Arcangeletti, M.C., Rodighiero, I., Buttrini, M., Montecchini, S., Vasile Simone, R., Medici, M.C., Chezzi, C., De Conto, F., 2016. Identification of different respiratory viruses, after a cell culture step, by matrix assisted laser desorption/ionization time of flight mass spectrometry (MALDI-TOF MS). Sci. Rep. 6, 36082. 〈https://doi.org/10.1038/srep36082〉.

Cao, G., Noti, J.D., Blachere, F.M., Lindsley, W.G., Beezhold, D.H., 2011. Development of an improved methodology to detect infectious airborne influenza virus using the NIOSH bioaerosol sampler. J. Environ. Monit. 13, 3321–3328. https://doi.org/10.1039/c1em10607d.

Cardozo, K.H.M., Lebkuchen, A., Okai, G.G., Schuch, R.A., Viana, L.G., Olive, A.N., dos, C., Lazari, S., Fraga, A.M., Granato, C.F.H., Pintão, M.C.T., Carvalho, V.M., 2020. Establishing a mass spectrometry-based system for rapid detection of SARS-CoV-2 in large clinical sample cohorts. Nat. Commun. 11, 1–13. https://doi.org/10.1038/s41467-020-19925-0.

CDC, 2021, Science Brief: SARS-CoV-2 and Surface (Fomite) Transmission for Indoor Community Environments - Updated Apr. 5, 2021.

Chaibun, T., Puenpa, J., Ngamdee, T., Boonapatcharoen, N., Athamanolap, P., O'Mullane, A.P., Vongpunsawad, S., Poovorawan, Y., Lee, S.Y., Lertanantawong, B., 2021. Rapid electrochemical detection of coronavirus SARS-CoV-2. Nat. Commun. 12, 802. https://doi.org/10.1038/s41467-021-21121-7.

Chang, C.W., Chou, F.C., 2011. Assessment of bioaerosol sampling techniques for viable Legionella pneumophila by ethidium monoazide quantitative PCR. Aerosol Sci. Technol. 45, 343–351. https://doi.org/10.1080/02786826.2010.537400.

Chan, V.W.M., So, S.Y.C., Chen, J.H.K., Yip, C.C.Y., Chan, K.H., Chu, H., Chung, T.W.H., Sridhar, S., To, K.K.W., Chan, J.F.W., Hung, I.F.N., Ho, P.L., Yuen, K.Y., 2020. Air and environmental sampling for SARS-CoV-2 around hospitalized patients with coronavirus disease 2019 (COVID-19). Infect. Control Hosp. Epidemiol. https://doi.org/10.1017/ice.2020.282.

Chen, H., Das, A., Bi, L., Choi, N., Il Moon, J., Wu, Y., Park, S., Choo, J., 2020. Recent advances in surface-enhanced Raman scattering-based microdevices for point-of-care diagnosis of viruses and bacteria. Nanoscale 12, 21560–21570. https://doi.org/10.1039/d0nr06340a.

Chia, P.Y., Coleman, K.K., Tan, Y.K., Ong, S.W.X., Gum, M., Lau, S.K., Lim, X.F., Lim, A. S., Sutjipto, S., Lee, P.H., Son, T.T., Young, B.E., Milton, D.K., Gray, G.C., Schuster, S., Barkham, T., De, P.P., Vasoo, S., Chan, M., Ang, B.S.P., Tan, B.H., Leo, Y.S., Ng, O.T., Wong, M.S.Y., Marimuthu, K., Lye, D.C., Lim, P.L., Lee, C.C., Ling, L.M., Lee, L., Lee, T.H., Wong, C.S., Sadarangani, S., Lin, R.J., Ng, D.H.L., Sadasiv, M., Yeo, T.W., Choy, C.Y., Tan, G.S.E., Dimatatac, F., Santos, I.F., Go, C.J., Chan, Y.K., Tay, J.Y., Tan, J.Y.L., Pandit, N., Ho, B.C.H., Mendis, S., Chen, Y.Y.C., Abdad, M.Y., Moses, D., 2020. Detection of air and surface contamination by SARS-CoV-2 in hospital rooms of infected patients. Nat. Commun. 11, 2800. https://doi.org/10.1038/s41467-020-16670-2.

Chirizzi, D., Conte, M., Feltracco, M., Dinoi, A., Gregoris, E., Barbaro, E., La Bella, G., Ciccarese, G., La Salandra, G., Gambaro, A., Contini, D., 2021. SARS-CoV-2 concentrations and virus-laden aerosol size distributions in outdoor air in north and south of Italy. Environ. Int. 146, 106255 https://doi.org/10.1016/j.envint.2020.106255.

Cho, Y.S., Hong, S.C., Choi, J., Jung, J.H., 2019. Development of an automated wet-cyclone system for rapid, continuous and enriched bioaerosol sampling and its application to real-time detection. Sens. Actuators, B Chem. https://doi.org/10.1016/j.snb.2018.12.155.

Christopher, M.W., GwangPyo, K., 2007, Effect of Ultraviolet Germicidal Irradiation on Viral Aerosols. 10.1021/ES070056U.

Cooper, C.D., Alley, F.C., 1986, Air pollution control: a design approach.

Cossart, P., Helenius, A., 2014. Endocytosis of viruses and bacteria. Cold Spring Harb. Perspect. Biol. 6 https://doi.org/10.1101/cshperspect.a016972.

van Doremalen, N., Bushmaker, T., Morris, D.H., Holbrook, M.G., Gamble, A., Williamson, B.N., Tamin, A., Harcourt, J.L., Thornburg, N.J., Gerber, S.I., Lloyd-Smith, J.O., de Wit, E., Munster, V.J., 2020. Aerosol and surface stability of SARS-CoV-2 as compared with SARS-CoV-1. N. Engl. J. Med. 382, 1564–1567. https://doi.org/10.1056/nejmc2004973.

Dumont-Leblond, N., Veillette, M., Mubareka, S., Yip, L., Longtin, Y., Jouvet, P., Paquet Bolduc, B., Godbout, S., Kobinger, G., McGeer, A., Mikszewski, A., Duchaine, C., 2020. Low incidence of airborne SARS-CoV-2 in acute care hospital rooms with optimized ventilation. Emerg. Microbes Infect. 9, 2597–2605. https://doi.org/10.1080/22221751.2020.1850184.

Dybwad, M., Skogan, G., Blatny, J.M., 2014. Comparative testing and evaluation of nine different air samplers: End-to-end sampling efficiencies as specific performance measurements for bioaerosol applications. Aerosol Sci. Technol. 48, 282–295. https://doi.org/10.1080/02786826.2013.871501.

Dziąbowska, K., Czaczyk, E., Nidzworski, D., 2018. Detection methods of human and animal influenza virus—current trends. Biosensors 8, 94. https://doi.org/10.3390/bios8040094.

Fabian, P., McDevitt, J.J., DeHaan, W.H., Fung, R.O.P., Cowling, B.J., Chan, K.H., Leung, G.M., Milton, D.K., 2008. Influenza virus in human exhaled breath: an observational study. PLoS One 3, 2691. https://doi.org/10.1371/journal.pone.0002691.

Fabian, P., McDevitt, J.J., Houseman, E.A., Milton, D.K., 2009. Airborne influenza virus detection with four aerosol samplers using molecular and infectivity assays:

considerations for a new infectious virus aerosol sampler. Indoor Air 19, 433–441. https://doi.org/10.1111/j.1600-0668.2009.00609.x.

Fennelly, K.P., 2020. Particle sizes of infectious aerosols: implications for infection control. Lancet Respir. Med. https://doi.org/10.1016/S2213-2600(20)30323-4.

Franchitti, E., Pascale, E., Fea, E., Anedda, E., Traversi, D., 2020. Methods for bioaerosol characterization: Limits and perspectives for human health risk assessment in organicwaste treatment. Atmosphere 11, 452. https://doi.org/10.3390/ATMOS11050452.

Fronczek, C.F., Yoon, J.-Y., 2015. Biosensors for monitoring airborne pathogens. J. Lab. Autom. 20, 390–410. https://doi.org/10.1177/2211068215580935.

Galbadage, T., Peterson, B.M., Gunasekera, R.S., 2020. Does COVID-19 spread through droplets alone? Front. Public Health 8. https://doi.org/10.3389/fpubh.2020.00163.

Ganguli, A., Mostafa, A., Berger, J., Aydin, M.Y., Sun, F., Stewart de Ramirez, S.A., Valera, E., Cunningham, B.T., King, W.P., Bashir, R., 2020. Rapid isothermal amplification and portable detection system for SARS-CoV-2. Proc. Natl. Acad. Sci. U. S. A. https://doi.org/10.1073/pnas.2014739117.

Ganova-Raeva, L.M., Khudyakov, Y.E., 2013. Application of mass spectrometry to molecular diagnostics of viral infections. Expert Rev. Mol. Diagn. 13, 377–388. https://doi.org/10.1586/erm.13.24.

Gelderblom, H.R., 1996, Structure and Classification of Viruses, University of Texas Medical Branch at Galveston. ⟨http://www.ncbi.nlm.nih.gov/pubmed/21413309⟩ (accessed 5 March 2020).

Ghosh, B., Lal, H., Srivastava, A., 2015a. Review of bioaerosols in indoor environment with special reference to sampling, analysis and control mechanisms. Environ. Int. 85, 254–272. https://doi.org/10.1016/J.ENVINT.2015.09.018.

Ghosh, B., Lal, H., Srivastava, A., 2015b. Review of bioaerosols in indoor environment with special reference to sampling, analysis and control mechanisms. Environ. Int. 85, 254–272. https://doi.org/10.1016/J.ENVINT.2015.09.018.

Ghosh, B., Lal, H., Srivastava, A., 2015c. Review of bioaerosols in indoor environment with special reference to sampling, analysis and control mechanisms. Environ. Int. 85, 254–272. https://doi.org/10.1016/j.envint.2015.09.018.

Gralton, J., Tovey, E., McLaws, M.L., Rawlinson, W.D., 2011. The role of particle size in aerosolised pathogen transmission: a review. J. Infect. 62, 1–13. https://doi.org/10.1016/j.jinf.2010.11.010.

Gralton, J., Tovey, E.R., Mclaws, M.L., Rawlinson, W.D., 2013. Respiratory virus RNA is detectable in airborne and droplet particles. J. Med. Virol. 85, 2151–2159. https://doi.org/10.1002/jmv.23698.

Guliy, O.I., Zaitsev, B.D., Larionova, O.S., Borodina, I.A., 2019. Virus detection methods and biosensor technologies. Biophys. (Russ. Fed. https://doi.org/10.1134/S0006350919060095.

Gupta, N., 2019. DNA extraction and polymerase chain reaction. J. Cytol. 36, 116–117. https://doi.org/10.4103/JOC.JOC_110_18.

Gupta, N., Augustine, S., Narayan, T., O'Riordan, A., Das, A., Kumar, D., Luong, J.H.T., Malhotra, B.D., 2021. Point-of-care PCR assays for COVID-19 detection. Biosensors 11. https://doi.org/10.3390/bios11050141.

Han, C.H., Ha, H.W., Jang, J., 2019. Two-dimensional computational method for generating planar electrode patterns with enhanced volumetric electric fields and its application to continuous dielectrophoretic bacterial capture. Lab Chip 19, 1772–1782. https://doi.org/10.1039/c8lc01288a.

Han, T.T., Thomas, N.M., Mainelis, G., 2017. Design and development of a self-contained personal electrostatic bioaerosol sampler (PEBS) with a wire-to-wire charger. Aerosol Sci. Technol. 51, 903–915. https://doi.org/10.1080/02786826.2017.1329516.

Han, C.H., Woo, S.Y., Bhardwaj, J., Sharma, A., Jang, J., 2018. Rapid and selective concentration of bacteria, viruses, and proteins using alternating current signal superimposition on two coplanar electrodes. Sci. Rep. https://doi.org/10.1038/s41598-018-33329-7.

Harvey, L., Arnold, B., Lawrence, Z.S., Pau, l.M., David, B., James, D., 2000, Molecular Cell Biology. 4th edition. https://doi.org/10.1016/j.jasms.2009.08.001.

Hill, S.C., Pan, Y.-L., Williamson, C., Santarpia, J.L., Hill, H.H., 2013. Fluorescence of bioaerosols: mathematical model including primary fluorescing and absorbing molecules in bacteria. Opt. Express 21, 22285–22313. https://doi.org/10.1364/oe.21.022285.

Hinds, W.C., 1999, Aerosol Technology Properties, behaviour, and Measurement if Airborne Particles.

Hogan, C.J., Kettleson, E.M., Lee, M.-H., Ramaswami, B., Angenent, L.T., Biswas, P., 2005. Sampling methodologies and dosage assessment techniques for submicrometre and ultrafine virus aerosol particles. J. Appl. Microbiol. 99, 1422–1434. https://doi.org/10.1111/j.1365-2672.2005.02720.x.

Hong, S., Bhardwaj, J., Han, C.-H., Jang, J., 2016. Gentle sampling of submicrometer airborne virus particles using a personal electrostatic particle concentrator. Environ. Sci. Technol. 50, 12365–12372. https://doi.org/10.1021/acs.est.6b03464.

Ho, J., 2011. Use of Virtual impactor (VI) technology in biological aerosol detection. KONA Powder Part. J. 29, 16–26. https://doi.org/10.14356/kona.2011006.

Huffman, J.A., Perring, A.E., Savage, N.J., Clot, B., Crouzy, B., Tummon, F., Shoshanim, O., Damit, B., Schneider, J., Sivaprakasam, V., Zawadowicz, M.A., Crawford, I., Gallagher, M., Topping, D., Doughty, D.C., Hill, S.C., Pan, Y., 2019. Real-time sensing of bioaerosols: review and current perspectives. Aerosol Sci. Technol. 1–31. https://doi.org/10.1080/02786826.2019.1664724.

Hu, J., Lei, C., 1#, C., Liu, W., Hu, X., Pei, R., Su, Z., Deng, F., Huang, Y., Sun, X., Cao, J., Guan, W., 2020a. Airborne SARS-CoV-2 and the use of masks for protection against its spread in Wuhan. China 1–16. ⟨https://www.nature.com/articles/d41586-020⟩.

Hu, J., Lei, C., Chen, Z., Liu, W., Hu, X., Pei, R., Su, Z., Deng, F., Huang, Y., Sun, X., Cao, J., Guan, W., 2020b. Distribution of airborne SARS-CoV-2 and possible aerosol transmission in Wuhan hospitals, China. Natl. Sci. Rev. 7, 1865–1867. https://doi.org/10.1093/nsr/nwaa250.

Ikonen, N., Savolainen-Kopra, C., Enstone, J.E., Kulmala, I., Pasanen, P., Salmela, A., Salo, S., Nguyen-Van-Tam, J.S., Ruutu, P., Gotcheva, N., Koivisto, R., Veijalainen, A. M., Poirot, N., Laajail, N., Bennett, E., Walters, C., Hall, I., Bastier, S., Lapeyre, Y., Berthier, A., 2018. Deposition of respiratory virus pathogens on frequently touched surfaces at airports. BMC Infect. Dis. 18, 437. https://doi.org/10.1186/s12879-018-3150-5.

Jiang, X., Loeb, J.C., Pan, M., Tilly, T.B., Eiguren-Fernandez, A., Lednicky, J.A., Wu, C.Y., Fan, Z.H., 2021. Integration of sample preparation with RNA-Amplification in a hand-held device for airborne virus detection. Anal. Chim. Acta 1165, 338542. https://doi.org/10.1016/j.aca.2021.338542.

Jiang, X., Pan, M., Hering, S.V., Lednicky, J.A., Wu, C.Y., Fan, Z.H., 2016. Use of RNA amplification and electrophoresis for studying virus aerosol collection efficiency and their comparison with plaque assays. Electrophoresis 37, 2574–2580. https://doi.org/10.1002/elps.201600141.

Ji, T., Liu, Z., Wang, G.Q., Guo, X., Akbar khan, S., Lai, C., Chen, H., Huang, S., Xia, S., Chen, B., Jia, H., Chen, Y., Zhou, Q., 2020. Detection of COVID-19: a review of the current literature and future perspectives. Biosens. Bioelectron. 166, 112455 https://doi.org/10.1016/j.bios.2020.112455.

Kabir, E., Azzouz, A., Raza, N., Bhardwaj, S.K., Kim, K.H., Tabatabaei, M., Kukkar, D., 2020. Recent advances in monitoring, sampling, and sensing techniques for bioaerosols in the atmosphere. ACS Sens. 5, 1254–1267. https://doi.org/10.1021/acssensors.9b02585.

Karimzadeh, S., Bhopal, R., Huy, N.T., 2021. Review of infective dose, routes of transmission, and outcome of COVID-19 caused by the SARS-COV-2: comparison with other respiratory viruses. Epidemiol. Infect. https://doi.org/10.1017/S0950268821000790.

Khalid Ijaz, M., Sattar, S.A., Rubino, J.R., Nims, R.W., Gerba, C.P., 2020. Combating SARS-CoV-2: leveraging microbicidal experiences with other emerging/re-emerging viruses. PeerJ 8, 9914. https://doi.org/10.7717/peerj.9914.

Khan, P., Aufdembrink, L.M., Engelhart, A.E., 2020. Isothermal SARS-CoV-2 diagnostics: tools for enabling distributed pandemic testing as a means of supporting safe reopenings. ACS Synth. Biol. 9, 2861–2880. https://doi.org/10.1021/acssynbio.0c00359.

Kim, H.R., An, S., Hwang, J., 2020a. Aerosol-to-hydrosol sampling and simultaneous enrichment of airborne bacteria for rapid biosensing. ACS Sens. https://doi.org/10.1021/acssensors.0c00555.

Kim, H.R., An, S., Hwang, J., 2020b. An integrated system of air sampling and simultaneous enrichment for rapid biosensing of airborne coronavirus and influenza virus. Biosens. Bioelectron. 170, 112656 https://doi.org/10.1016/j.bios.2020.112656.

Kim, H.R., An, S., Hwang, J., 2021. High air flow-rate electrostatic sampler for the rapid monitoring of airborne coronavirus and influenza viruses. J. Hazard. Mater. 412, 125219 https://doi.org/10.1016/j.jhazmat.2021.125219.

King, M.D., Lacey, R.E., Pak, H., Fearing, A., Ramos, G., Baig, T., Smith, B., Koustova, A., 2020. Assays and enumeration of bioaerosols-traditional approaches to modern practices. Aerosol Sci. Technol. 54, 611–633. https://doi.org/10.1080/02786826.2020.1723789.

Knudsen, R.C., 2001. Alcohol consumption is associated with reduced prevalence of goitre and solitary thyroid nodules. Clin. Endocrinol. (Oxf.) 55, 41–46. https://doi.org/10.1177/153567600100600106.

Kulkarni, H., Smith, C.M., Lee, D.D.H., Hirst, R.A., Easton, A.J., O'Callaghan, C., 2016. Evidence of respiratory syncytial virus spread by aerosol time to revisit infection control strategies? Am. J. Respir. Crit. Care Med. 194, 308–316. https://doi.org/10.1164/rccm.201509-1833OC.

Kwon, H.-J., Fronczek, C.F., Angus, S.V., Nicolini, A.M., Yoon, J.-Y., 2014. Rapid and sensitive detection of H1N1/2009 virus from aerosol samples with a microfluidic immunosensor. J. Lab. Autom. 19, 322–331. https://doi.org/10.1177/2211068213504205.

Ladhani, L., Pardon, G., Meeuws, H., van Wesenbeeck, L., Schmidt, K., Stuyver, L., van der Wijngaart, W., 2017. Sampling and detection of airborne influenza virus towards point-of-care applications. PLoS One 12, 0174314. https://doi.org/10.1371/journal.pone.0174314.

Lednicky, J.A., Lauzard, M., Fan, Z.H., Jutla, A., Tilly, T.B., Gangwar, M., Usmani, M., Shankar, S.N., Mohamed, K., Eiguren-Fernandez, A., Stephenson, C.J., Alam, M.M., Elbadry, M.A., Loeb, J.C., Subramaniam, K., Waltzek, T.B., Cherabuddi, K., Morris, J. G., Wu, C.Y., 2020. Viable SARS-CoV-2 in the air of a hospital room with COVID-19 patients. Int. J. Infect. Dis. 100, 476–482. https://doi.org/10.1016/j.ijid.2020.09.025.

Lednicky, J.A., Loeb, J.C., 2013. Detection and isolation of airborne influenza A H3N2 virus using a sioutas personal cascade impactor sampler. Influenza Res. Treat. 2013, 656825 https://doi.org/10.1155/2013/656825.

Lednicky, J., Pan, M., Loeb, J., Hsieh, H., Eiguren-Fernandez, A., Hering, S., Fan, Z.H., Wu, C.-Y., 2016. Highly efficient collection of infectious pandemic influenza H1N1 virus (2009) through laminar-flow water based condensation. Aerosol Sci. Technol. 50, i–iv. https://doi.org/10.1080/02786826.2016.1179254.

Lee, J., Jang, J., Akin, D., Savran, C.A., Bashir, R., 2008. Real-time detection of airborne viruses on a mass-sensitive device. Appl. Phys. Lett. 93, 13901. https://doi.org/10.1063/1.2956679.

Lee, I., Seok, Y., Jung, H., Yang, B., Lee, J., Kim, J., Pyo, H., Song, C.S., Choi, W., Kim, M. G., Lee, J., 2020. Integrated bioaerosol sampling/monitoring platform: field-deployable and rapid detection of airborne viruses. ACS Sens. 5, 3915–3922. https://doi.org/10.1021/acssensors.0c01531.

Leung, N.H.L., Zhou, J., Chu, D.K.W., Yu, H., Lindsley, W.G., Beezhold, D.H., Yen, H.L., Li, Y., Seto, W.H., Peiris, J.S.M., Cowling, B.J., 2016. Quantification of influenza virus RNA in aerosols in patient rooms. PLoS One. https://doi.org/10.1371/journal.pone.0148669.

Lindsley, W.G., Blachere, F.M., Thewlis, R.E., Vishnu, A., Davis, K.A., Cao, G., Palmer, J. E., Clark, K.E., Fisher, M.A., Khakoo, R., Beezhold, D.H., 2010. Measurements of airborne influenza virus in aerosol particles from human coughs. PLoS One 5, 15100. https://doi.org/10.1371/journal.pone.0015100.

Lindsley, W.G., Schmechel, D., Chen, B.T., 2006. A two-stage cyclone using microcentrifuge tubes for personal bioaerosol sampling. J. Environ. Monit. 8, 1136–1142. https://doi.org/10.1039/b609083d.

Lin, X.T., Hsu, N.Y., Wang, J.R., Chen, N.T., Su, H.J., Lin, M.Y., 2018. Development of an efficient viral aerosol collector for higher sampling flow rate. Environ. Sci. Pollut. Res. https://doi.org/10.1007/s11356-017-0754-z.

Lippe, R., 2019, Flow virometry: a powerful tool to functionally characterize, Virology.

Liu, Y., Ning, Z., Chen, Y., Guo, M., Liu, Y., Gali, N.K., Sun, L., Duan, Y., Cai, J., Westerdahl, D., Liu, X., Xu, K., fai Ho, K., Kan, H., Fu, Q., Lan, K., 2020. Aerodynamic analysis of SARS-CoV-2 in two Wuhan hospitals. Nature. https://doi.org/10.1038/s41586-020-2271-3.

Li, J., Leavey, A., Wang, Y., O'Neil, C., Wallace, M.A., Burnham, C.A.D., Boon, A.C., Babcock, H., Biswas, P., 2018. Comparing the performance of 3 bioaerosol samplers for influenza virus. J. Aerosol Sci. 115, 133–145. https://doi.org/10.1016/j.jaerosci.2017.08.007.

Lv, J., Yang, J., Xue, J., Zhu, P., Liu, L., Li, S., 2020. Detection of SARS-CoV-2 RNA residue on object surfaces in nucleic acid testing laboratory using droplet digital PCR. Sci. Total Environ. 742, 140370 https://doi.org/10.1016/j.scitotenv.2020.140370.

Mainelis, G., 2020. Bioaerosol sampling: classical approaches, advances, and perspectives. Aerosol Sci. Technol. 54, 496–519. https://doi.org/10.1080/02786826.2019.1671950.

Marple, V.A., Willeke, K., 1976. Impactor design. Atmos. Environ. (1967) 10, 891–896. https://doi.org/10.1016/0004-6981(76)90144-X.

Masri, N.M., Hanbali, L.B., Kamar, A.H., Kanafani, L.M.S., Hanbali, M.B., Haddad, J.J., 2013. The immunomodulatory, antimicrobial and bactericidal efficacy of commonly used commercial household disinfectants, sterilizers and antiseptics *in vitro*: putative anti-inflammatory infection control mechanisms and comparative biochemic. Am. J. Med. Biol. Res. https://doi.org/10.12691/ajmbr-1-4-4.

McDevitt, J.J., Koutrakis, P., Ferguson, S.T., Wolfson, J.M., Fabian, M.P., Martins, M., Pantelic, J., Milton, D.K., 2013. Development and performance evaluation of an exhaled-breath bioaerosol collector for influenza virus. Aerosol Sci. Technol. 47, 444–451. https://doi.org/10.1080/02786826.2012.762973.

Milewska, A., Ner-Kluza, J., Dabrowska, A., Bodzon-Kulakowska, A., Pyrc, K., Suder, P., 2020. Mass spectrometry in virological sciences. Mass Spectrom. Rev. 39, 499–522. https://doi.org/10.1002/mas.21617.

Milton, D.K., Fabian, M.P., Cowling, B.J., Grantham, M.L., McDevitt, J.J., 2013. Influenza virus aerosols in human exhaled breath: particle size, culturability, and effect of surgical masks. PLoS Pathog. 9, 1003205 https://doi.org/10.1371/journal.ppat.1003205.

Mo, Y., Wan, R., Zhang, Q., 2012. Application of reverse transcription-PCR and real-time PCR in nanotoxicity research. Methods Mol. Biol. 926, 99–112. https://doi.org/10.1007/978-1-62703-2-1_7.

Myatt, T.A., Johnston, S.L., Rudnick, S., Milton, D.K., 2003. Airborne rhinovirus detection and effect of ultraviolet irradiation on detection by a semi-nested RT-PCR assay. BMC Public Health 3, 5. https://doi.org/10.1186/1471-2458-3-5.

Nissen, K., Krambrich, J., Akaberi, D., Hoffman, T., Ling, J., Lundkvist, Å., Svensson, L., Salaneck, E., 2020. Long-distance airborne dispersal of SARS-CoV-2 in COVID-19 wards. Sci. Rep. 10, 19589. https://doi.org/10.1038/s41598-020-76442-2.

Noti, J.D., Lindsley, W.G., Blachere, F.M., Cao, G., Kashon, M.L., Thewlis, R.E., McMillen, C.M., King, W.P., Szalajda, J.V., Beezhold, D.H., 2012. Detection of infectious influenza virus in cough aerosols generated in a simulated patient examination room. Clin. Infect. Dis. 54, 1569–1577. https://doi.org/10.1093/cid/cis237.

Oh, S., Anwar, D., Theodore, A., Lee, J.H., Wu, C.Y., Wander, J., 2010. Development and evaluation of a novel bioaerosol amplification unit (BAU) for improved viral aerosol collection. J. Aerosol Sci. 41, 889–894. https://doi.org/10.1016/j.jaerosci.2010.06.002.

Oishee, M.J., Ali, T., Jahan, N., Khandker, S.S., Haq, M.A., Khondoker, M.U., Sil, B.K., Lugova, H., Krishnapillai, A., Abubakar, A.R., Kumar, S., Haque, M., Jamiruddin, M. R., Adnan, N., 2021. Covid-19 pandemic: review of contemporary and forthcoming detection tools. Infect. Drug Resist. 14, 1049–1082. https://doi.org/10.2147/IDR.S289629.

Oppliger, A., Masclaux, F.G., Niculita-Hirzel, H., 2011. Assessment of airborne microorganisms by real-time PCR optimistic findings and research challenges. Front Biosci. S3, 445–453. https://doi.org/10.2741/s163.

Owen, T.W., Al-Kaysi, R.O., Bardeen, C.J., Cheng, Q., 2007. Microgravimetric immunosensor for direct detection of aerosolized influenza A virus particles. Sens. Actuators B: Chem. 126, 691–699. https://doi.org/10.1016/j.snb.2007.04.028.

Pan, M., Bonny, T.S., Loeb, J., Jiang, X., Lednicky, J.A., Eiguren-Fernandez, A., Hering, S., Fan, Z.H., Wu, C.-Y., 2017. Collection of viable aerosolized influenza virus and other respiratory viruses in a student health care center through water-based condensation growth. MSphere 2. https://doi.org/10.1128/mSphere.00251-17.

Pan, M., Eiguren-Fernandez, A., Hsieh, H., Afshar-Mohajer, N., Hering, S.V., Lednicky, J., Hugh Fan, Z., Wu, C.Y., 2016. Efficient collection of viable virus aerosol through laminar-flow, water-based condensational particle growth. J. Appl. Microbiol. 120, 805–815. https://doi.org/10.1111/jam.13051.

Pan, M., Lednicky, J.A., Wu, C. -Y., 2019. Collection, particle sizing and detection of airborne viruses. J. Appl. Microbiol. 127, 1596–1611. https://doi.org/10.1111/jam.14278.

Park, K.-T., Cho, D.-G., Park, J.-W., Hong, S., Hwang, J., 2015. Detection of airborne viruses using electro-aerodynamic deposition and a field-effect transistor. Sci. Rep. 5, 17462. https://doi.org/10.1038/srep17462.

Piri, A., Kim, H.R., Park, D.H., Hwang, J., 2021. Increased survivability of coronavirus and H1N1 influenza virus under electrostatic aerosol-to-hydrosol sampling. J. Hazard. Mater. 413, 125417 https://doi.org/10.1016/j.jhazmat.2021.125417.

Price, R.H.M., Graham, C., Ramalingam, S., 2019. Association between viral seasonality and meteorological factors. Sci. Rep. 9, 929. https://doi.org/10.1038/s41598-018-37481-y.

Prussin, A.J., Garcia, E.B., Marr, L.C., 2015. Total virus and bacteria concentrations in indoor and outdoor air. Environ. Sci. Technol. Lett. 2, 84–88. https://doi.org/10.1021/acs.estlett.5b00050.

Prussin, A.J., Marr, L.C., Bibby, K.J., 2014. Challenges of studying viral aerosol metagenomics and communities in comparison with bacterial and fungal aerosols. FEMS Microbiol. Lett. 357, 1–9. https://doi.org/10.1111/1574-6968.12487.

Rahmani, A.R., Leili, M., Azarian, G., Poormohammadi, A., 2020. Sampling and detection of corona viruses in air: a mini review. Sci. Total Environ. 740, 140207 https://doi.org/10.1016/j.scitotenv.2020.140207.

Ribeiro, B.V., Cordeiro, T.A.R., Oliveira e Freitas, G.R., Ferreira, L.F., Franco, D.L., 2020. Biosensors for the detection of respiratory viruses: a review. Talanta Open 2, 100007. https://doi.org/10.1016/j.talo.2020.100007.

Rosenthal, K.S., Tan, M.J., Rosenthal, K.S., 2011. Rapid Review Microbiology and Immunology. Mosby/Elsevier.

Rule, A.M., Kesavan, J., Schwab, K.J., Buckley, T.J., 2007. Application of flow cytometry for the assessment of preservation and recovery efficiency of bioaerosol samplers spiked with Pantoea agglomerans. Environ. Sci. Technol. 41, 2467–2472. https://doi.org/10.1021/es062394l.

Sagripanti, J.L., Lytle, C.D., 2020. Estimated inactivation of coronaviruses by solar radiation with special reference to COVID-19. Photochem. Photobiol. 96, 731–737. https://doi.org/10.1111/php.13293.

Sakudo, A., Onodera, T., Tanaka, Y., 2011. Inactivation of viruses. Steriliz. Disinfect. Plasma Steriliz. Mech. Biol. Med. Appl. https://doi.org/10.1016/b978-1-4832-2765-8.50011-7.

Salari, A., Thompson, M., 2018. Recent advances in AC electrokinetic sample enrichment techniques for biosensor development. Sens. Actuators B: Chem. 255, 3601–3615. https://doi.org/10.1016/j.snb.2017.09.069.

Santarpia, J.L., Herrera, V.L., Rivera, D.N., Ratnesar-Shumate, S., Reid, S.P., Denton, P. W., Martens, J.W.S., Fang, Y., Conoan, N., Callahan, M.V., Lawler, J.V., Brett-Major, D.M., Lowe, J.J., 2020, The infectious nature of patient-generated SARS-CoV-2 aerosol, MedRxiv. https://doi.org/10.1101/2020.07.13.20041632.

Santarpia, J., Rivera, D., Herrera, V., Morwitzer, M.J., Creager, H., Santarpia, G., Crown, K., Brett-Major, D., Schnaubelt, E., Broadhurst, M.J., Lawler, J., Reid, S., Lowe, J., 2020, Aerosol and Surface Transmission Potential of SARS-CoV-2, MedRxiv.

Schrader, C., Schielke, A., Ellerbroek, L., Johne, R., 2012. PCR inhibitors – occurrence, properties and removal. J. Appl. Microbiol. 113, 1014–1026. https://doi.org/10.1111/j.1365-2672.2012.05384.x.

Sengupta, A., Brar, N., Davis, E.J., 2007. Bioaerosol detection and characterization by surface-enhanced Raman spectroscopy. J. Colloid Interface Sci. 309, 36–43. https://doi.org/10.1016/j.jcis.2007.02.015.

Sengupta, A., Laucks, M.L., Dildine, N., Drapala, E., Davis, E.J., 2005. Bioaerosol characterization by surface-enhanced Raman spectroscopy (SERS). J. Aerosol Sci. 36, 651–664. https://doi.org/10.1016/j.JAEROSCI.2004.11.001.

Sharma Ghimire, P., Tripathee, L., Chen, P., Kang, S., 2019. Linking the conventional and emerging detection techniques for ambient bioaerosols: a review. Rev. Environ. Sci. Bio/Technol. 18, 495–523. https://doi.org/10.1007/s11157-019-09506-z.

Shen, F., Tan, M., Wang, Z., Yao, M., Xu, Z., Wu, Y., Wang, J., Guo, X., Zhu, T., 2011a. Integrating silicon nanowire field effect transistor, microfluidics and air sampling techniques for real-time monitoring biological aerosols. Environ. Sci. Technol. 45, 7473–7480. https://doi.org/10.1021/es1043547.

Shen, F., Tan, M., Wang, Z., Yao, M., Xu, Z., Wu, Y., Wang, J., Guo, X., Zhu, T., 2011b. Integrating silicon nanowire field effect transistor, microfluidics and air sampling techniques for real-time monitoring biological aerosols. Environ. Sci. Technol. 45, 7473–7480. https://doi.org/10.1021/es1043547.

Shen, F., Wang, J., Xu, Z., Wu, Y., Chen, Q., Li, X., Jie, X., Li, L., Yao, M., Guo, X., Zhu, T., 2012. Rapid flu diagnosis using silicon nanowire sensor. Nano Lett. 12, 3722–3730. https://doi.org/10.1021/nl301516z.

, 1995Spieksma, F.T.M., Bioaerosols Handbook. Edited by C. S. Cox and C. M. Wathes. Boca Raton & London: CRC/Lewis (1995), pp. 623, £58.00. ISBN 1–87371-615–9, Exp. Agric. (1997). https://doi.org/10.1017/s0014479792220223.

Su, X., Sutarlie, L., Loh, X.J., 2020. Sensors and analytical technologies for air quality: particulate matters and bioaerosols. Chem. Asian J. 15, 4241–4255. https://doi.org/10.1002/asia.202001051.

Tang, J.W., 2009. The effect of environmental parameters on the survival of airborne infectious agents. J. R. Soc. Interface 6 (Suppl 6), S737–S746. https://doi.org/10.1098/rsif.2009.0227.focus.

Tan, C., Fan, D., Wang, N., Wang, F., Wang, B., Zhu, L., Guo, Y., 2021. Applications of digital PCR in COVID-19 pandemic. View. https://doi.org/10.1002/viw.20200082.

Tellier, R., Li, Y., Cowling, B.J., Tang, J.W., 2019. Recognition of aerosol transmission of infectious agents: a commentary. BMC Infect. Dis. 19, 101. https://doi.org/10.1186/s12879-019-3707-y.

Tellier, R., 2009. Aerosol transmission of influenza A virus: a review of new studies. J. R. Soc. Interface 6 (Suppl 6), S783–S790. https://doi.org/10.1098/rsif.2009.0302.focus.

Tirella, P.N., Craig, R.L., Tubbs, D.B., Olson, N.E., Lei, Z., Ault, A.P., 2018. Extending surface enhanced Raman spectroscopy (SERS) of atmospheric aerosol particles to the

accumulation mode (150–800 nm). Environ. Sci. Process. Impacts 20, 1570–1580. https://doi.org/10.1039/c8em00276b.

Tseng, C.C., Li, C.S., 2005. Collection efficiencies of aerosol samplers for virus-containing aerosols. J. Aerosol Sci. 36, 593–607. https://doi.org/10.1016/j.jaerosci.2004.12.004.

Turgeon, N., McNicoll, F., Toulouse, M.J., Liav, A., Barbeau, J., Ho, J., Grund, C., Duchaine, C., 2011. Neuraminidase activity as a potential enzymatic marker for rapid detection of airborne viruses. Aerosol Sci. Technol. 45, 183–195. https://doi.org/10.1080/02786826.2010.530624.

Uk Lee, B., Jung, J.H., Yun, S.H., Hwang, G.B., Bae, G.N., 2010. Application of UVAPS to real-time detection of inactivation of fungal bioaerosols due to thermal energy. J. Aerosol Sci. 41, 694–701. https://doi.org/10.1016/j.jaerosci.2010.04.003.

Usachev, E.V., Agranovski, I.E., 2012. Internally controlled PCR system for detection of airborne microorganisms. J. Environ. Monit. 14, 1631. https://doi.org/10.1039/c2em30019b.

Usachev, E.V., Agranovski, E., Usacheva, O.V., Agranovski, I.E., 2015. Multiplexed surface plasmon resonance based real time viral aerosol detection. J. Aerosol Sci. 90, 136–143. https://doi.org/10.1016/J.JAEROSCI.2015.08.009.

Usachev, E.V., Pankova, A.V., Rafailova, E.A., Pyankov, O.V., Agranovski, I.E., 2012. Portable automatic bioaerosol sampling system for rapid on-site detection of targeted airborne microorganisms. J. Environ. Monit. 14, 2739–2745. https://doi.org/10.1039/c2em30317e.

Usachev, E.V., Tam, A.M., Usacheva, O.V., Agranovski, I.E., 2014. The sensitivity of surface plasmon resonance based viral aerosol detection. J. Aerosol Sci. 76, 39–47. https://doi.org/10.1016/J.JAEROSCI.2014.05.004.

Usachev, E.V., Usacheva, O.V., Agranovski, I.E., 2013. Surface plasmon resonance-based real-time bioaerosol detection. J. Appl. Microbiol. 115, 766–773. https://doi.org/10.1111/jam.12267.

Vasickova, P., Pavlik, I., Verani, M., Carducci, A., 2010. Issues concerning survival of viruses on surfaces. Food Environ. Virol. 2, 24–34. https://doi.org/10.1007/s12560-010-9025-6.

Verreault, D., Moineau, S., Duchaine, C., 2008. Methods for sampling of airborne viruses. Microbiol. Mol. Biol. Rev. 72, 413–444. https://doi.org/10.1128/MMBR.00002-08.

Verreault, D., Rousseau, G.M., Gendron, L., Massé, D., Moineau, S., Duchaine, C., 2010. Comparison of polycarbonate and polytetrafluoroethylene filters for sampling of airborne bacteriophages. Aerosol Sci. Technol. 44, 197–201. https://doi.org/10.1080/02786820903518899.

Walls, H.J., Ensor, D.S., Harvey, L.A., Kim, J.H., Chartier, R.T., Hering, S.V., Spielman, S. R., Lewis, G.S., 2016. Generation and sampling of nanoscale infectious viral aerosols. Aerosol Sci. Technol. 50, 802–811. https://doi.org/10.1080/02786826.2016.1191617.

Walther, B.A., Ewald, P.W., 2004. Pathogen survival in the external environment and the evolution of virulence. Biol. Rev. Camb. Philos. Soc. 79, 849–869. https://doi.org/10.1017/S1464793104006475.

Wang, C.-H., Tschen, S.-Y., Flehmig, B., 1995. Antigenicity of hepatitis A virus after ultra-violet inactivation. Vaccine 13, 835–840. https://doi.org/10.1016/0264-410X(94)00054-Q.

Watanabe, T., Bartrand, T.A., Weir, M.H., Omura, T., Haas, C.N., 2010. Development of a dose-response model for SARS coronavirus. Risk Anal. 30, 1129–1138. https://doi.org/10.1111/j.1539-6924.2010.01427.x.

Whon, T.W., Kim, M.-S., Roh, S.W., Shin, N.-R., Lee, H.-W., Bae, J.-W., 2012. Metagenomic characterization of airborne viral DNA diversity in the near-surface atmosphere. J. Virol. 86, 8221–8231. https://doi.org/10.1128/jvi.00293-12.

William, N., Lindsley, G., Green, B.J., Blachere, F.M., Martin, S.B., Law, B.F., Jensen, P. A., Schafer, M.P., 2017. Sampling and characterization of bioaerosols. NIOSH Man. Anal. Methods BA–2-BA-115.

Wilson, N.M., Norton, A., Young, F.P., Collins, D.W., 2020. Airborne transmission of severe acute respiratory syndrome coronavirus-2 to healthcare workers: a narrative review. Anaesthesia 75, 1086–1095. https://doi.org/10.1111/anae.15093.

Xu, Z., Wu, Y., Shen, F., Chen, Q., Tan, M., Yao, M., 2011. Bioaerosol science, technology, and engineering: past, present, and future. Aerosol Sci. Technol. 45, 1337–1349. https://doi.org/10.1080/02786826.2011.593591.

Yang, W., Elankumaran, S., Marr, L.C., 2011. Concentrations and size distributions of airborne influenza A viruses measured indoors at a health centre, a day-care centre and on aeroplanes. J. R. Soc. Interface 8, 1176–1184. https://doi.org/10.1098/rsif.2010.0686.

Yan, J., Grantham, M., Pantelic, J., Bueno de Mesquita, P.J., Albert, B., Liu, F., Ehrman, S., Milton, N.K., EMIT Consortium, 2018. Infectious virus in exhaled breath of symptomatic seasonal influenza cases from a college community. Proc. Natl. Acad. Sci. U. S. A. 115, 1081–1086. https://doi.org/10.1073/pnas.1716561115.

Yezli, S., Otter, J.A., 2011. Minimum infective dose of the major human respiratory and enteric viruses transmitted through food and the environment. Food Environ. Virol. 3, 1–30. https://doi.org/10.1007/s12560-011-9056-7.

Yoon, S.N., Lee, J., Kim, D., Yoo, H.S., Min, K.Y., Kim, M.C., 2019. The use of LIF-based instrument with 405 nm for real-time monitoring of aerosolized bio-particles. JKSAE 13, 186–195. https://doi.org/10.5572/ajae.2019.13.3.186.

Zhao, Y., Aarnink, A.J.A., Wang, W., Fabri, T., Groot Koerkamp, P.W.G., de Jong, M.C. M., 2014. Airborne virus sampling: efficiencies of samplers and their detection limits for infectious bursal disease virus (IBDV). Ann. Agric. Environ. Med. 21, 464–471. https://doi.org/10.5604/12321966.1120585.

Zhen, H., Han, T., Fennell, D.E., Mainelis, G., 2013. Release of free DNA by membrane-impaired bacterial aerosols due to aerosolization and air sampling. Appl. Environ. Microbiol. 79, 7780–7789. https://doi.org/10.1128/AEM.02859-13.

Zukeran, A., Sawano, H., Ito, K., Oi, R., Kobayashi, I., Wada, R., Sawai, J., 2018. Investigation of inactivation process for microorganism collected in an electrostatic precipitator. J. Electrost. 93, 70–77. https://doi.org/10.1016/j.elstat.2018.04.002.

Šantl-Temkiv, T., Sikoparija, B., Maki, T., Carotenuto, F., Amato, P., Yao, M., Morris, C. E., Schnell, R., Jaenicke, R., Pöhlker, C., DeMott, P.J., Hill, T.C.J., Huffman, J.A., 2020. Bioaerosol field measurements: challenges and perspectives in outdoor studies. Aerosol Sci. Technol. 54, 520–546. https://doi.org/10.1080/02786826.2019.1676395.